

Aircraft Obstruction of Microwave Links

R. E. Skerjanec

R. W. Hubbard



U.S. DEPARTMENT OF COMMERCE
Juanita M. Kreps, Secretary

Henry Geller, Assistant Secretary
for Communications and Information

January 1979



TABLE OF CONTENTS

	Page
ABSTRACT	1
1. INTRODUCTION	2
2. PHYSICAL DESCRIPTION	3
3. MEASUREMENT CONFIGURATION	10
4. RECEIVED SIGNAL LEVEL ANALYSIS	20
5. IMPULSE RESPONSE ANALYSIS	29
5.1. Hartsfield-Atlanta International Airport	34
5.2. O'Hare-Chicago International Airport	38
6. CONCLUSIONS AND RECOMMENDATIONS	44
7. ACKNOWLEDGMENTS	47
8. REFERENCES	47
APPENDIX - Explanation of Impulse Test Data	48
REFERENCES	57

LIST OF FIGURES

	Page
Figure 2.1. Plan view of Hartsfield Atlanta International Airport.	4
Figure 2.2. Atlanta transmitting antennas.	5
Figure 2.3. Atlanta receiving antennas on control tower.	6
Figure 2.4. Profile of Atlanta path.	7
Figure 2.5. Plan view of O'Hare Chicago International Airport.	8
Figure 2.6. Chicago transmitting antenna configuration.	9
Figure 2.7. Chicago receiving antennas.	11
Figure 2.8. Chicago microwave path.	12
Figure 2.9. Profile of Chicago path.	13
Figure 3.1. Block diagram of the PN probe transmitter at 8.6 GHz.	15
Figure 3.2. The theoretical line spectrum of a pseudo-random binary signal.	15
Figure 3.3. The measured power spectrum (in dB) of the transmitted signal of the PN probe operating at a clock frequency of 150 MHz. The center frequency is 8.6 GHz, and the frequency scale is 50 MHz per division.	17
Figure 3.4. Block diagram of the PN probe receiver.	19
Figure 4.1. Aircraft fades for select periods.	21
Figure 4.2. Aircraft fade (Atlanta).	23
Figure 4.3. Aircraft position in microwave path.	24
Figure 4.4. Aircraft position above microwave path.	25
Figure 4.5. Aircraft position below microwave path.	26
Figure 4.6. Long duration fade at Chicago.	28
Figure 4.7. Aircraft orientation at Atlanta.	30

	Page
Figure 4.8. Multiple short duration fades at Chicago.	31
Figure 4.9. Multiple mixed fades at Chicago.	32
Figure 4.10. Time expanded fade at Chicago.	33
Figure 5.1. A typical response measured over the reflected (Channel B) link at the Atlanta airport without aircraft interference.	35
Figure 5.2. The impulse response measured at the Atlanta airport with a DC9 aircraft in the microwave beam. The time separation in (a) is 100 ms. The data rate in (b) 50 impulses per second.	35
Figure 5.3. Examples of the impulse response measured at the Atlanta airport with 727 aircraft intercepting the microwave beam. In (a) the aircraft was approaching Runway 27R, and in (b) it was approaching Runway 27L. The time between responses is 100 ms in each case.	37
Figure 5.4. A sequence of impulse responses measured over the Chicago-O'Hare RML link with no aircraft interference.	37
Figure 5.5. A typical response measured over the Chicago-O'Hare link with an aircraft obstruction.	40
Figure 5.6. A sequence of impulse responses measured during an obstruction fade. Multipath is seen in the fourth trace from the top.	40
Figure 5.7. Multipath observations over the Chicago-O'Hare link.	42
Figure 5.8. An obstruction fade without multipath.	43
Figure A-1. Time and frequency domain displays.	49
Figure A-2. The theoretical transfer function of a multipath channel.	52



AIRCRAFT OBSTRUCTION OF MICROWAVE LINKS

R.E. Skerjanec and R.W. Hubbard*

Conversion to digital transmission has renewed the concerns about what effects aircraft obstruction of microwave links have on user quality. This is of particular concern where it is necessary to install a telecommunication system that crosses runways and taxiways where the frequency of obstruction may be great.

A limited measurement program at 8 GHz at Atlanta and Chicago Airports was undertaken to determine if a condition existed that could cause excessive error rates on digital systems. Measurements were made of the received signal level together with the impulse response of the transmission medium.

Measurement results indicate that during takeoff and landing, aircraft can cause signal level fades to 20 dB. Modern system margin is usually sufficient to cope with such fades.

The impulse response measurements at Atlanta did not reveal any delayed or distorted pulses that would indicate excessive multipath and frequency selective fading. However, slight distortion from taxiing aircraft at Chicago was observed. The implication of this detected distortion is reflected in the potential of a distorted asymmetrical frequency response within the 15 - 20 MHz passband of a microwave digital receiver.

Key words: Microwave propagation; impulse response; digital transmission; aircraft obstruction

*The authors are with the Institute for Telecommunication Sciences, National Telecommunications and Information Administration, U.S. Department of Commerce, Boulder, Colorado 80303.

AIRCRAFT OBSTRUCTION OF MICROWAVE LINKS

1. INTRODUCTION

Recurrent situations arise when it is necessary for a variety of reasons to establish a line-of-sight microwave link at or near airports. Engineering questions often arise because of this situation. Do aircraft, when they are near the microwave link, cause a disturbance in the transmission of information? If so, what are the engineering trade-offs available to the designer? The superficial answer may be that there is little or no effect on analog information transmission when the user terminal has a long time constant or persistence or the refresh rate is not critical. This type of effect may not be important but because of the apparent lack of published data, it is quite possible that expensive overdesign has resulted.

Recent trends in wideband microwave transmission have been toward digital transmission. Data rates of interest are in the 12 to 50 Mb/s range. If such a system were implemented across a runway, the expected short disturbances could have a more profound effect than they might have with analog information.

The Army Communications Command contracted the Institute for Telecommunication Sciences to perform a limited measurement program to obtain data on an established system and to form some conclusion on whether a design problem exists and what its magnitude may be or whether it could be ignored. The basic question to be addressed was whether a large aircraft in its normal operation was sufficient to cause near total microwave beam blockage or sufficient multipath to cause phase and frequency distortion to result in a significant disturbance in the information baseband.

A measurement program was undertaken at two locations. The international airports at Atlanta, Georgia and Chicago, Illinois both had microwave links crossing active runways and taxiways. Permission was granted by the Federal Aviation Administration Regional Offices to utilize these links.

2. PHYSICAL DESCRIPTION

The microwave links of interest were established to remote airport surveillance radar (ASR-7) video to the control tower for use in airport control. A plan view of the microwave links at the Atlanta airport is shown in Figure 2.1. The direct path goes from the ASR-7 radar site to the control tower and is 0.8 miles (1.3 km) in length. The indirect route goes from the ASR-7 site to a passive reflector on a water tower at a height of 40 ft (12 m) and then to the control tower. Those distances are approximately 2.6 (4.2 km) and 2.3 miles (3.7 km) respectively. The transmitting antenna is approximately 19 ft (5.8 m) above ground level and the receiving antenna on the control tower is approximately 265 ft (80.8 m) above ground level. A view of the transmitting antenna is shown in Figure 2.2 and the receiving antenna in Figure 2.3. The relative locations between the runways and taxiways and the microwave terminals are shown in Figure 2.4 for the link that goes directly from the radar to the control tower. In examining this figure, one should be aware of a large vertical exaggeration and in fact the left-most runway is only 90 ft (27.4 m) below the microwave beam. For perspective, the tail height of a Boeing 747 aircraft is 63 ft (19.2 m) above ground.

The physical orientation of the two links is such that the probability of the same aircraft intersecting both microwave routes is nearly zero. When aircraft land from the east, the approach may intersect the indirect route but aircraft taking off from the east are normally not airborne at the direct microwave route. If operations are from the west, the landing aircraft are normally down and rolling below the microwave beam, whereas the aircraft taking off will on occasion intersect the direct microwave beam.

Similarly, the Chicago, Illinois airport is shown in Figure 2.5. The transmitting antennas are shown in Figure 2.6. These antennas have a horizontal separation of approximately 95 ft (29 m) providing horizontal space diversity rather than



Figure 2.2. Atlanta transmitting antennas.



Figure 2.3. Atlanta receiving antennas on control tower.

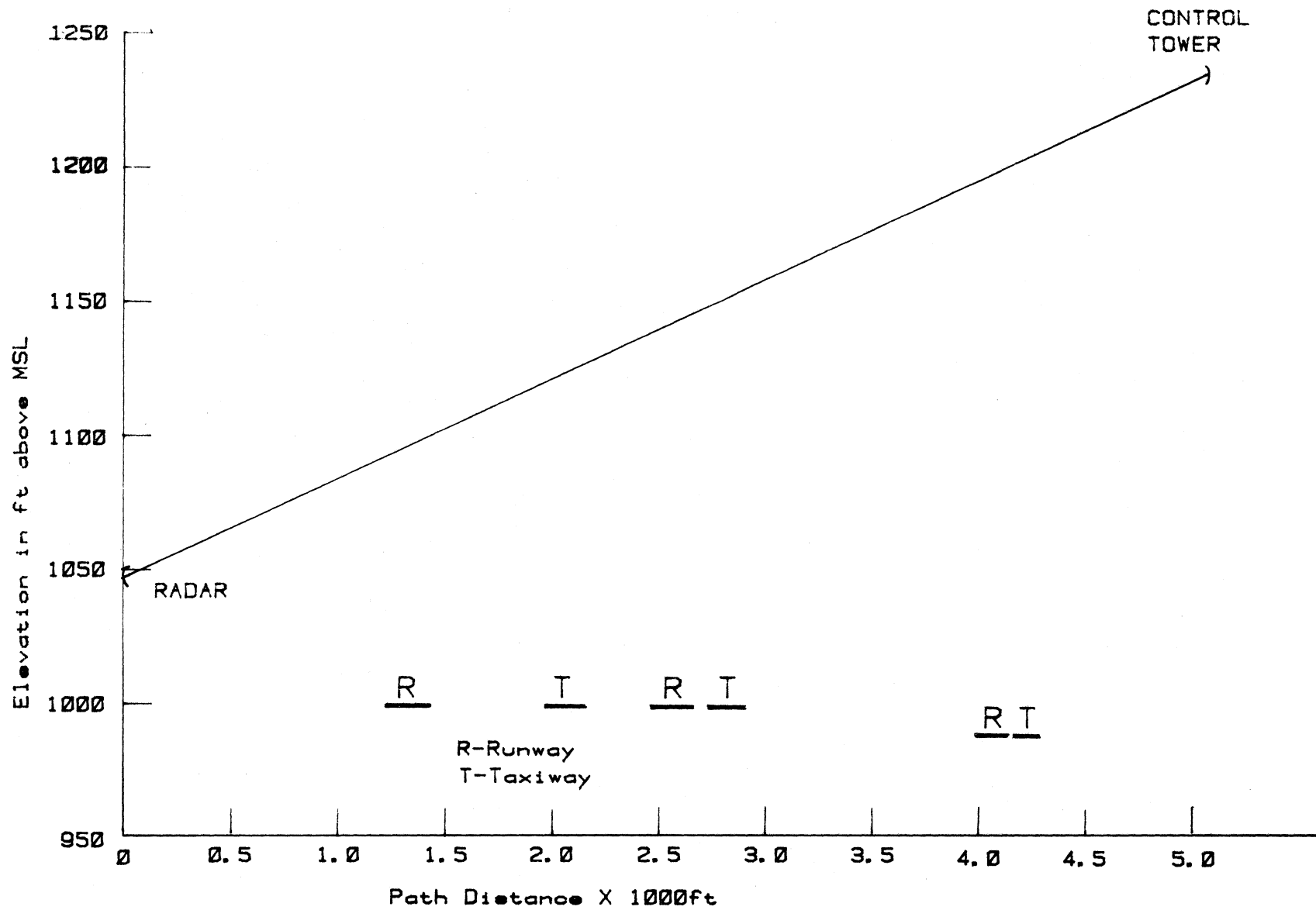


Figure 2.4. Profile of Atlanta path.

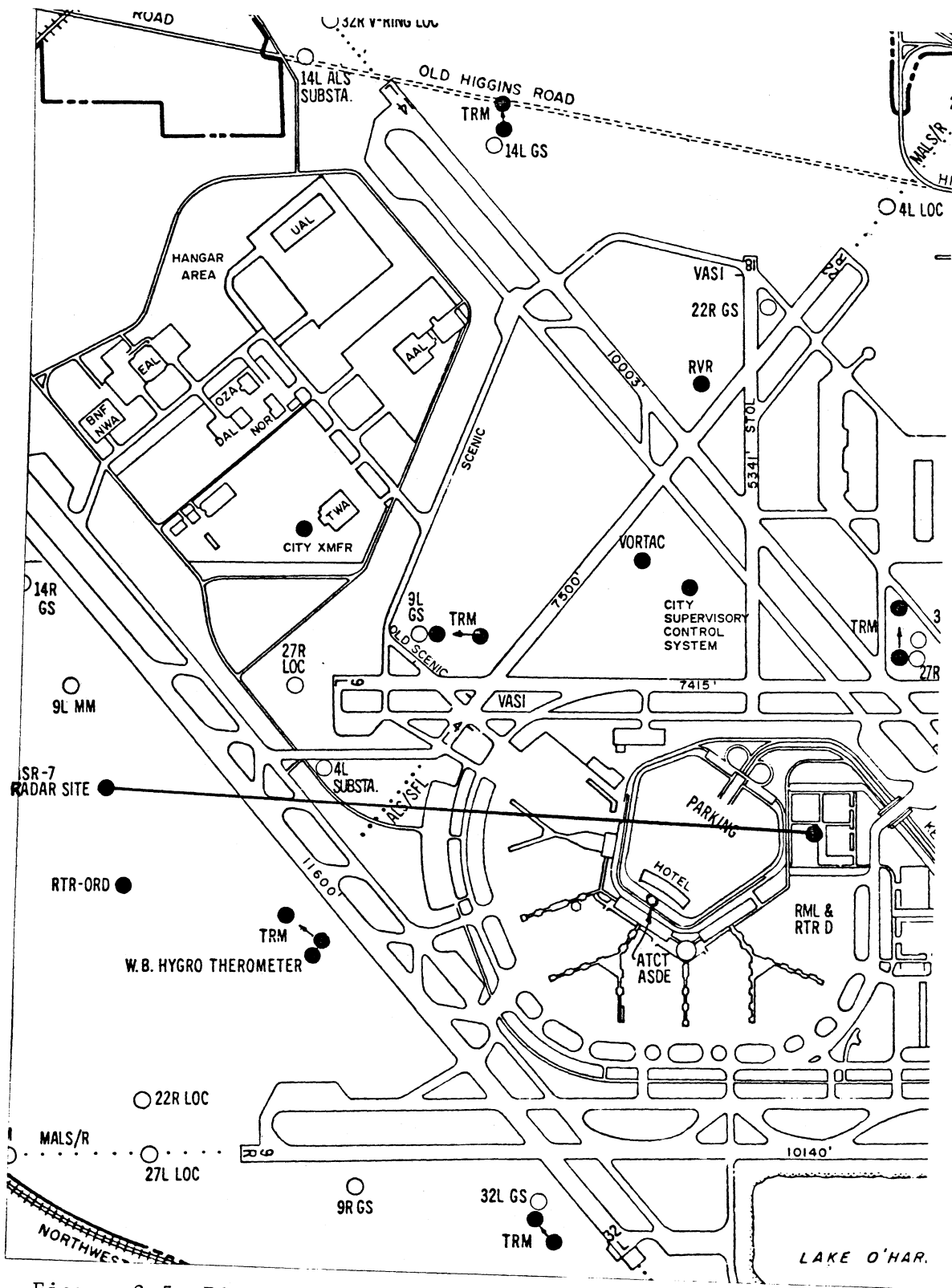


Figure 2.5 Plan view of O'Hare Chicago International Airport.

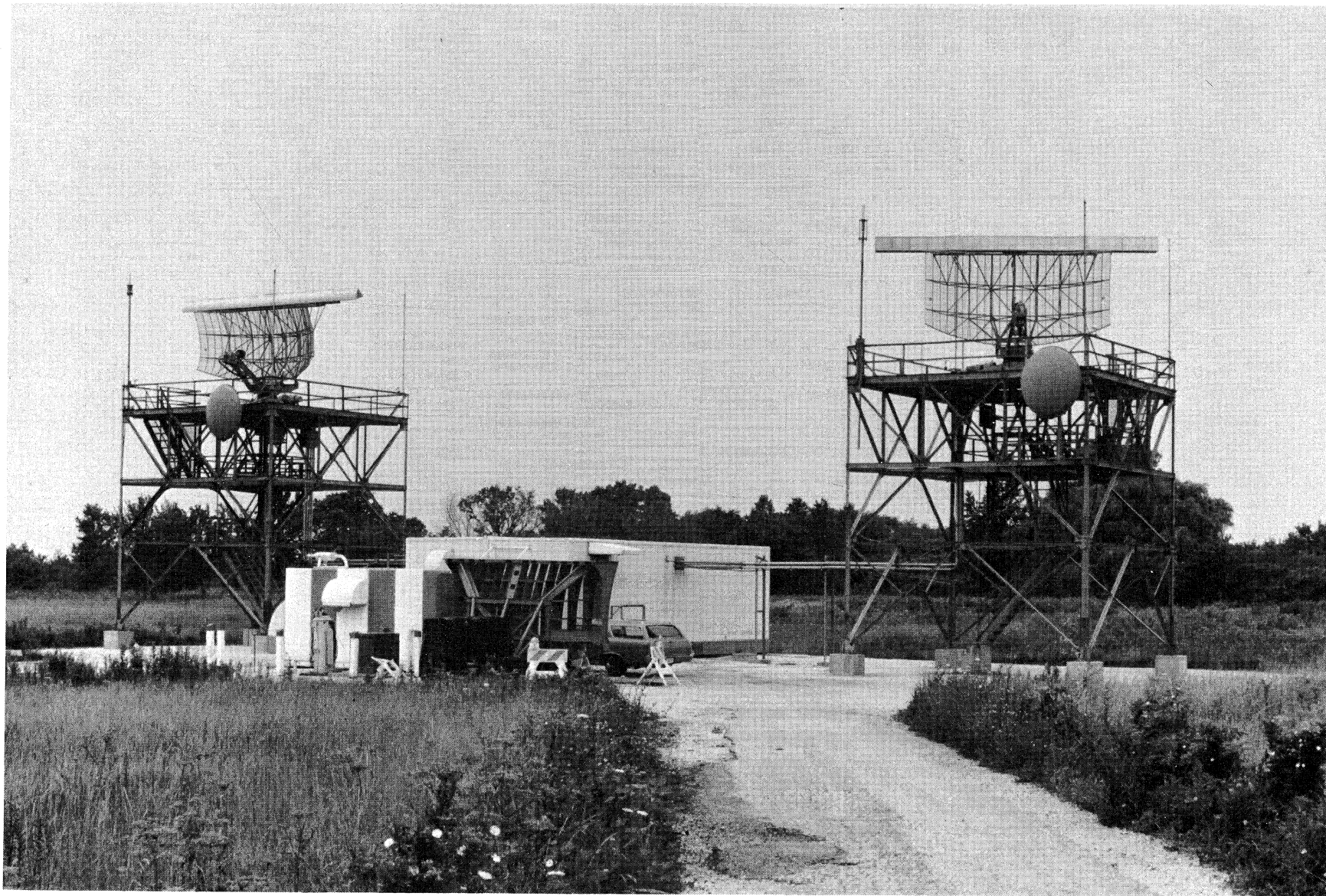


Figure 2.6. Chicago transmitting antenna configuration.

route diversity described above for the Atlanta airport. The receiving antennas are the two side-by-side dishes near the top of the tower in Figure 2.7. A view of the path is shown in Figure 2.8 from ground level near the transmitting terminal. The radar microwave link (RML) tower can be seen behind the center of the aircraft. A profile view is given in Figure 2.9 showing the relative locations of the runways, taxiways, and antenna terminals. The runway on the left of the figure is approximately 40 ft (12 m) below the microwave path. This provides the opportunity for the tail sections of the jumbo-jet class of aircraft to intersect or partially obstruct the microwave path.

The path is so oriented that it crosses the runway near the middle as shown in Figure 2.5. Operations from either direction would affect the system in a similar way. That is, aircraft taking off would normally be airborne by the time they reach the microwave path. They normally have sufficient height to clear the path, although a small percentage do intersect. On the other hand, aircraft landing have touched down by the time they reach the microwave path but the clearance is such that there would be some effects from the aircraft tails.

3. MEASUREMENT CONFIGURATION

With permission and access received from the Federal Aviation Administration, measurements were made at the Chicago and Atlanta commercial airports. The measurements were made from a twofold approach. The first was to gather path amplitude variability data from the AGC circuits on the existing RML-6 systems. The purpose of this segment was to obtain the path-loss data over a dynamic range commensurate with a standard microwave receiver and to obtain these data within the limitation of the AGC response time of the receiver system.

The second approach was to utilize a channel probe that is a separate stand-alone element containing the transmit and receive functions and requiring only the use of the transmission lines and antennas of the existing FAA system.

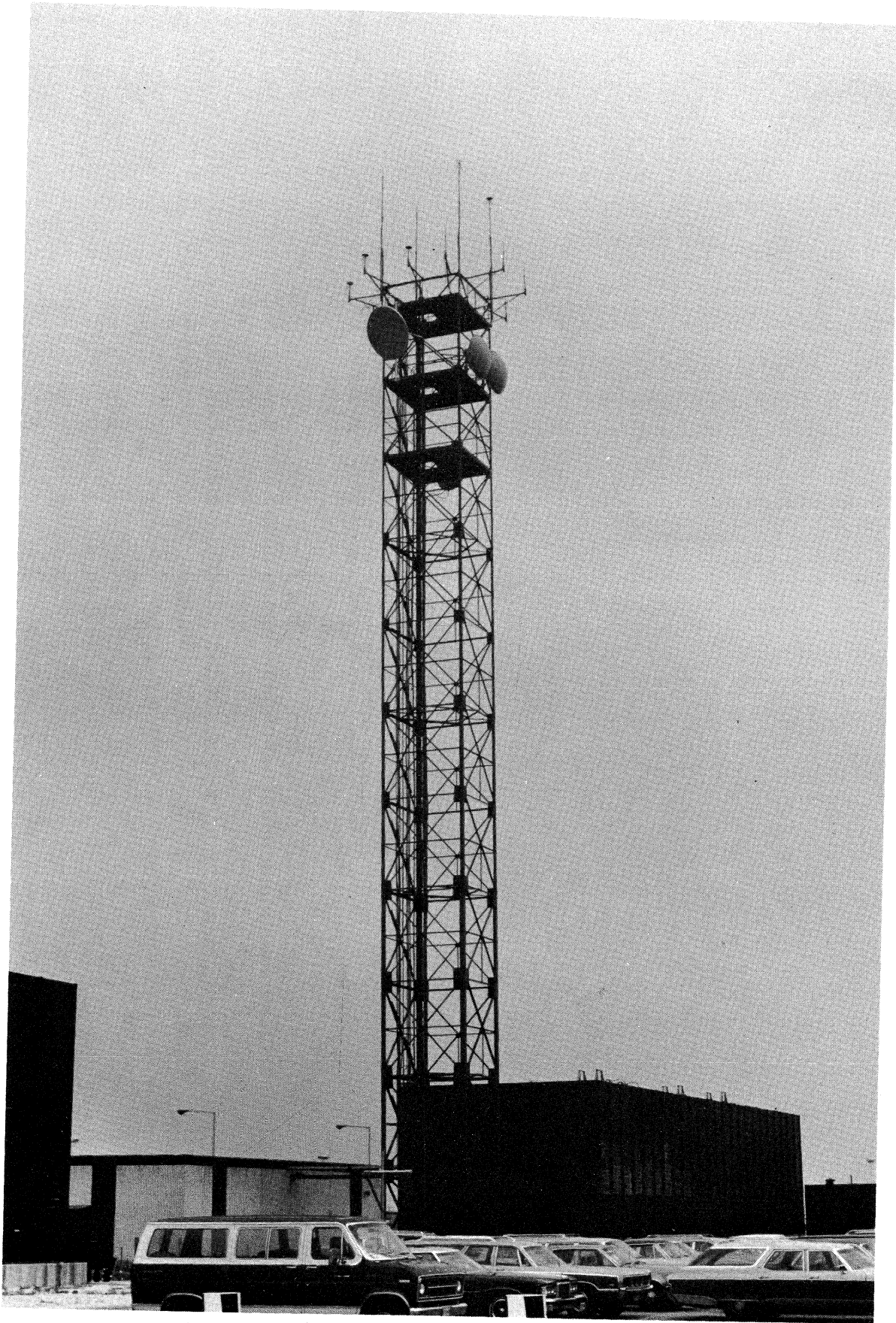


Figure 2.7. Chicago receiving antennas.

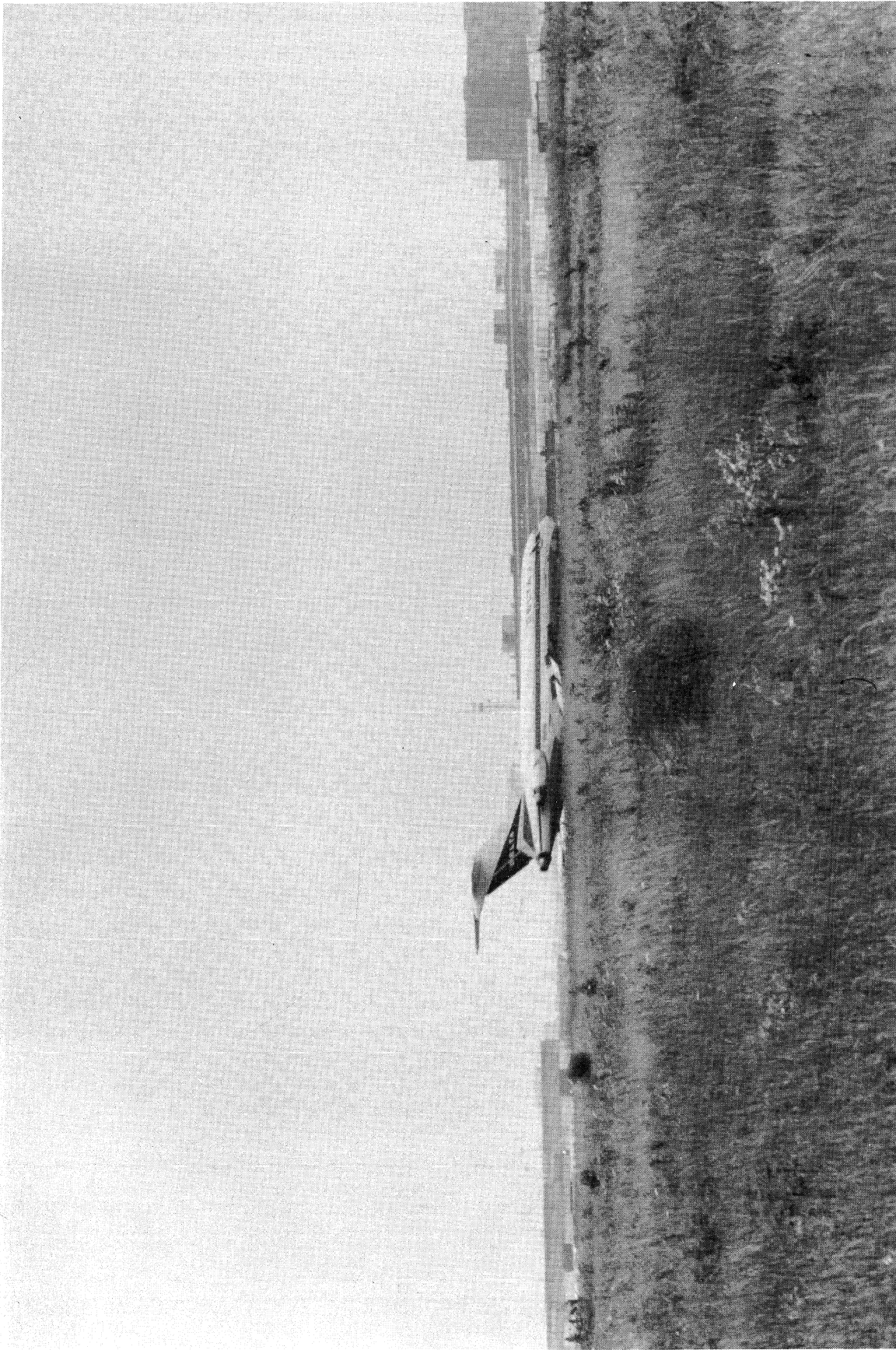


Figure 2.8. Chicago microwave path.

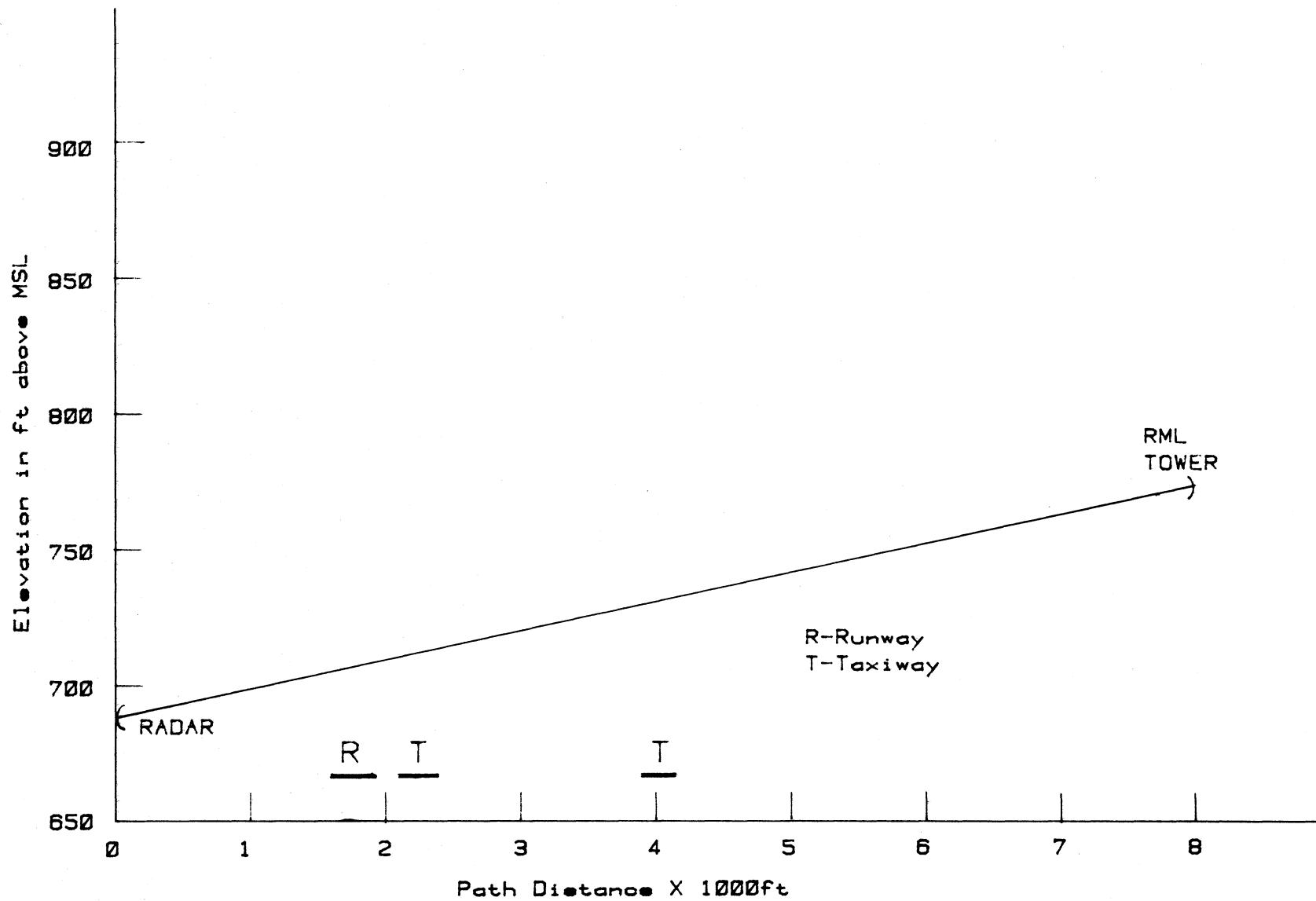


Figure 2.9. Profile of Chicago path.

The received signal level data and the baseband noise were recorded on an FM analog tape recorder and monitored by an appropriate strip chart recorder. The tape recorder was capable of recording changes of 625 Hz. This can be translated to a time constant of 1.6 ms for full scale changes. Measurements were to be made for a one-week period at each of the two airports. Recording of the parameters was accompanied by visual observation of the various aircraft at Atlanta. The recording facilities at Chicago were beyond sight of the runways so visual observations could not be made.

A wideband channel probe system developed at ITS for evaluating multipath conditions in microwave and other radio propagation links was used in the test program (Linfield et al., 1976).

This system transmits (in the normal operating mode) a wideband pseudo-random binary bit stream as a test signal, which results in a radiated signal at 8.6 GHz that resembles pseudo-random noise (PN). The binary code is generated from a 9-stage shift register with feedback, providing an optimal length pseudo-random stream of 511 bits. The bit stream is clocked at a rate of 150 MHz.

The following is provided to convey the probe operational details, including power budget, spectrum and frequency assignment considerations.

Figure 3.1 shows a block diagram of the pseudo-random noise (PN) probe transmitter. The reference source is a 5 MHz stable oscillator that is used to develop both the IF (600 MHz) and the rf radiated signal.

The 600 MHz IF signal is bi-phase modulated with the PN binary sequence, which is clocked at $f = 150$ MHz rate.

The 5 MHz reference frequency is multiplied to an rf of 8 GHz, and is mixed in a double-balanced circuit with the 600 MHz IF signal. This produces a double-sideband suppressed carrier signal with the two sidebands centered at 7.4 GHz and 8.6 GHz. The rf filter shown in the block diagram of Figure 3.1

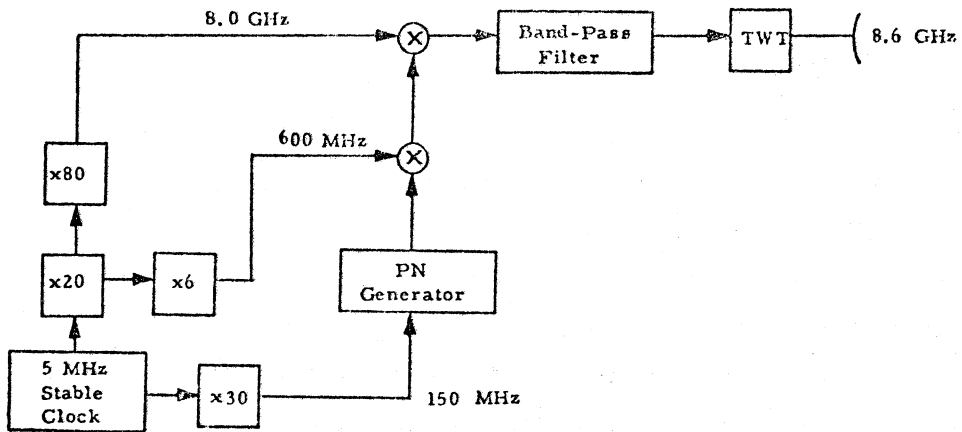


Figure 3.1. Block diagram of the PN probe transmitter at 8.6 GHz.

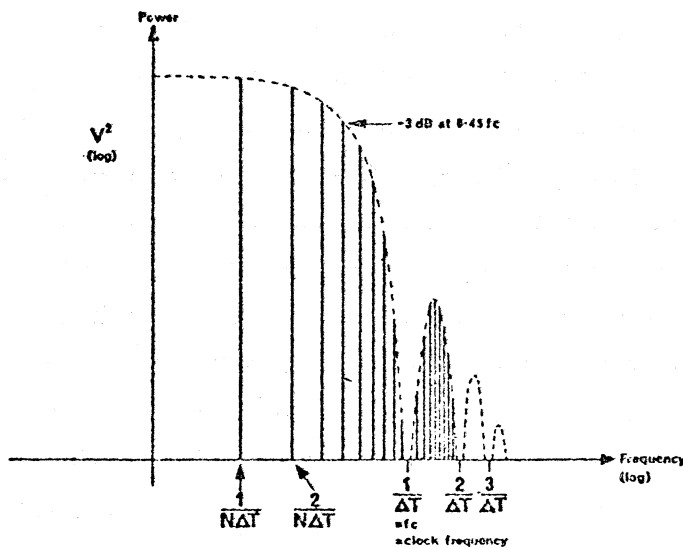


Figure 3.2. The theoretical line spectrum of a pseudo-random binary signal.

is used to pass only the upper sideband, and reject the lower. Therefore, the radiated signal is centered at the 8.6 GHz frequency.

The spectrum of a PN binary signal is a line spectrum, with power concentrated at frequencies given by $K/N\Delta T$ where

N = length of PN sequence in bits

ΔT = clock period ($1/f_c$)

K = harmonic number.

From this, it is seen that the power occurs at intervals of $1/N\Delta T$. The envelope of this line spectrum has the shape of $(\sin x/x)^2$, with nulls occurring at intervals of $1/\Delta T$. The primary power is thus concentrated in the first lobe of the envelope, with the first null at

$$1/(\Delta T) = f_c = 150 \text{ MHz.}$$

This spectrum function is illustrated in Figure 3.2. The PN signal bi-phase modulates the 600 MHz IF signal, producing the spectrum of the PN signal centered around 600 MHz. The spectrum of the radiated signal is the double-sided spectrum of that illustrated in Figure 3.2, centered at 8.6 GHz.

The rf filter is designed to shape the final spectrum around 8.6 GHz, attenuating the secondary lobes of the $(\sin x/x)^2$ envelope. The spectrum as measured over a transmission link, is shown in the photograph of Figure 3.3, taken from the display scope of a spectrum analyzer.

The maximum power capability of the probe transmitter is that of the TWT amplifier used in the final stage. This is rated at approximately 15 watts. However, this power level was not required on any of the test links. The transmitter power was held to the minimum level that was commensurate with the path loss and the receiver sensitivity for each link.

The radiated signal of the probe system resembles a random Gaussian noise with fairly uniform power density. The power is distributed over an approximate bandwidth of 300 MHz. Therefore, if this signal were detected by a narrow-band system,

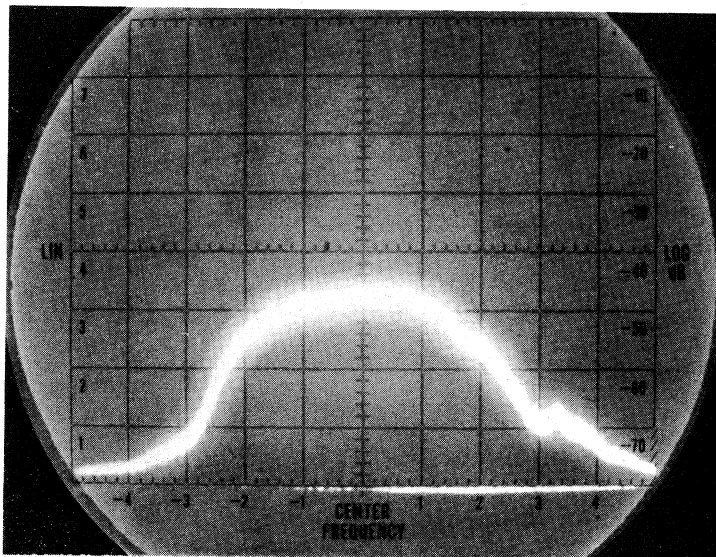


Figure 3.3. The measured power spectrum (in dB) of the transmitted signal of the PN probe operating at a clock frequency of 150 MHz. The center frequency is 8.6 GHz, and the frequency scale is 50 MHz per division.

it would not normally be a serious source of interference. It would result only in a slight increase in background noise level in the narrow-band system. For example, assuming complete uniform power density over the proposed 300 MHz bandwidth, and the maximum power from the transmitter of 1.5 watts, the power per unit frequency would be approximately:

$$\begin{aligned}\text{Trans. Power Density} &= 1500 \text{ mW}/300 \text{ MHz} \\ &= 5 \times 10^{-6} \text{ mW/Hz.}\end{aligned}$$

Using the gain at 8.6 GHz for a 6 ft (1.8 m) parabolic antenna (41.5 dB), the above power density would result in an ERP density of:

$$\begin{aligned}\text{ERP Power Density} &= 5 \times 10^{-6} \times 14,125 \\ &= 0.07 \text{ mW/Hz.}\end{aligned}$$

The receiver of the probe system is shown in Figure 3.4 in block diagram form. The received signal is correlated with a co- and quad-phase replica of the transmitted signal, at the IF of 600 MHz. The relative phases of the received components are then determined from the quadrature signals developed by the correlation detectors. These quadrature functions are squared and combined in the receiver to provide a direct output of the impulse magnitude. The output of the receiver is the impulse response of the transmission channel. The 600 MHz IF signal is monitored with a power meter, and is recorded through a log converter amplifier for received signal level (RSL) measurement. All four of these output signals are recorded on analog magnetic tape for future analyses. The quadrature or magnitude impulse response functions are monitored in real time on an oscilloscope during measurement. In addition, the RSL is recorded on a strip-chart recorder for direct comparison with the impulse data.

The receiver is designed for self-calibration. A locally generated 8.6 GHz PN modulated signal is fed to the rf head of the system, and measured with a power meter at the 600 MHz IF

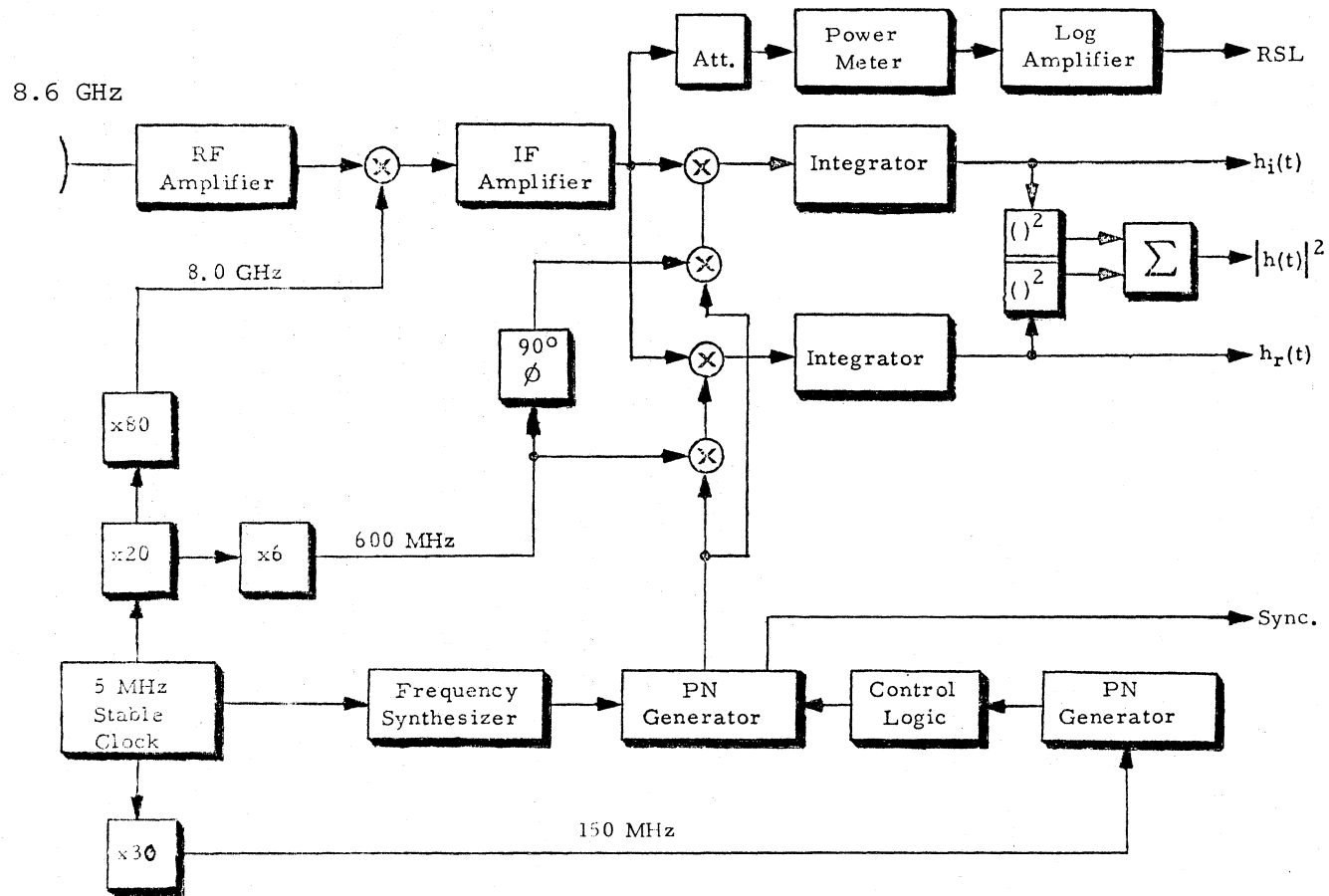


Figure 3.4. Block diagram of the PN probe receiver.

for a reference level (both RSL and impulse magnitude). Step attenuators in the rf head are then used to calibrate the receiver over the dynamic range. Transmitter power is measured directly with a power meter at the 8.6 GHz output of the TWT amplifier. All line losses at both the 8.6 GHz rf and 600 MHz IF were measured prior to link measurements, and accounted for in the system calibration.

The recorded data included the following:

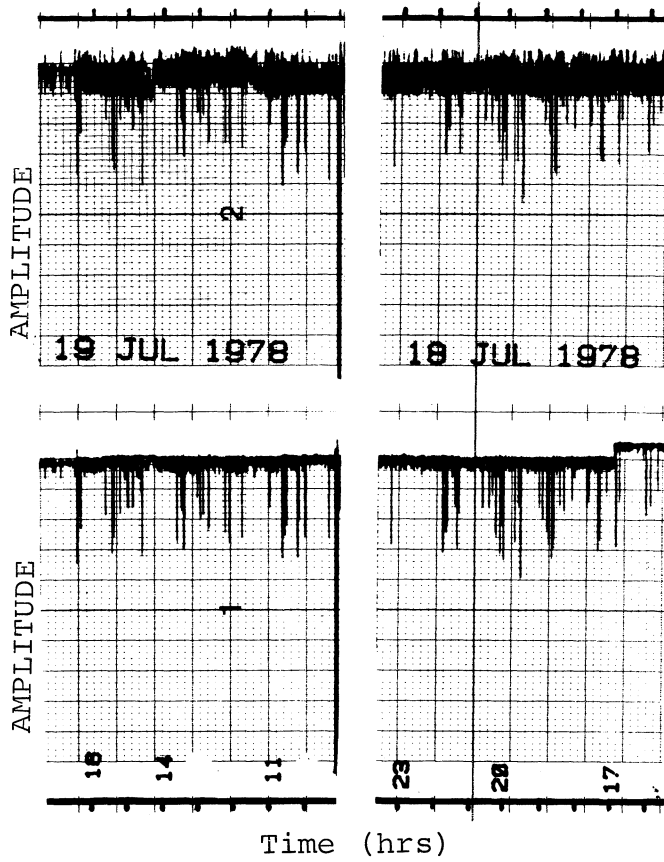
1. Co-phase impulse
2. Quad-phase impulse
3. Power impulse
4. Sync. pulse
5. Time code
6. IF RSL

These data were recorded on magnetic tape for playback and analyses in the ITS laboratories.

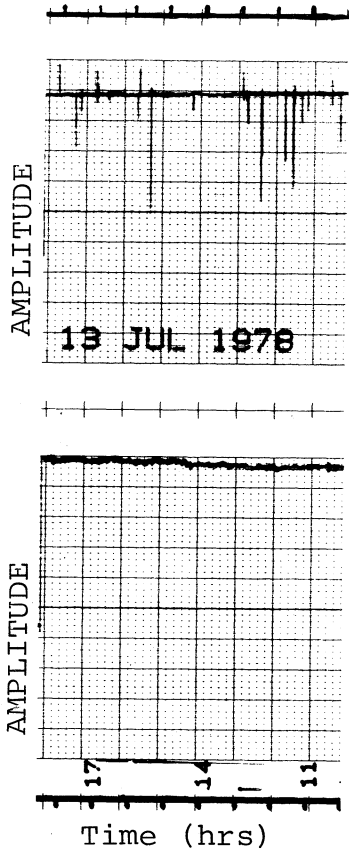
4. RECEIVED SIGNAL LEVEL ANALYSIS

As detailed in the previous section one phase of the data acquisition was the recording of the AGC voltages on the FAA RML-6 receivers. The segments of strip-chart recordings in Figure 4.1 are a time compression of select periods during data acquisition at Chicago and Atlanta. This figure is intended to illustrate the density of aircraft-microwave beam intersections. The Atlanta data indicates about four occurrences per hour as typical and Chicago data indicate a frequency of up to eight per hour. Further, in the same figure one can get a feel for the variance in the depth of fades.

As a first step in the analysis, the strip-chart recordings were reviewed and each case of a significant fade was time tagged and the depth of fade hand scaled from the chart. The depth of fade in this case is defined as the difference in signal level between that immediately prior to the aircraft detection and the minimum signal level.



CHICAGO



ATLANTA

Figure 4.1. Aircraft fades for select periods.

For the recording period between 11 July 1978 and 14 July 1978 at Atlanta Hartsfield Airport, 87 cases of fades caused by aircraft were identified on the strip-chart recording. Of these, 38 were detected on the A Receiver, the direct link between the radar and tower. The median for this data group is 6 dB and the mean is 7 dB. The deepest fade detected was on the order of 18 dB.

In addition to recording the AGC voltage, the combiner control voltage driven by a baseband noise sensor in the RML-6 equipment was monitored. No direct means was readily available to calibrate this function but as a function of received signal level, output changes were not detected until the input signal level dropped to -45 dBm to -50 dBm. This is used as an indication of excessive noise in the baseband. Only on the occasion of the three deepest fades was any measurable change noted, and then only approximately a 5-dB increase in baseband noise. The general appearance for the Atlanta configuration is that fades do occur but at moderate depths and with little disturbance to the baseband signal-to-noise ratio.

Figure 4.2 shows the characteristic of the deepest fade (18 dB) that was recorded at Atlanta. The A Receiver designation is for the direct link from transmitter to receiver. The duration is about 0.5 s with the bottom displaying two distinct nulls. These null pairs will be shown later to be common and possibly suggestive of separate fuselage and tail obstructions. The leading edge of the fade shows about 13 dB change in 1/8 s suggesting an approximate fade rate of 100 dB/s.

Figures 4.3 through 4.5 are taken to illustrate three aircraft positions with respect to the microwave path. The view is from the control tower toward the transmitting antenna marked by the arrow in all three figures. In Figure 4.3, the aircraft is completely obstructing the transmitting antenna causing one of the observed fades. Figure 4.4 illustrates an aircraft near but above the microwave path resulting in a limited shallow fade. The L-1011 jumbo jet in Figure 4.5 can

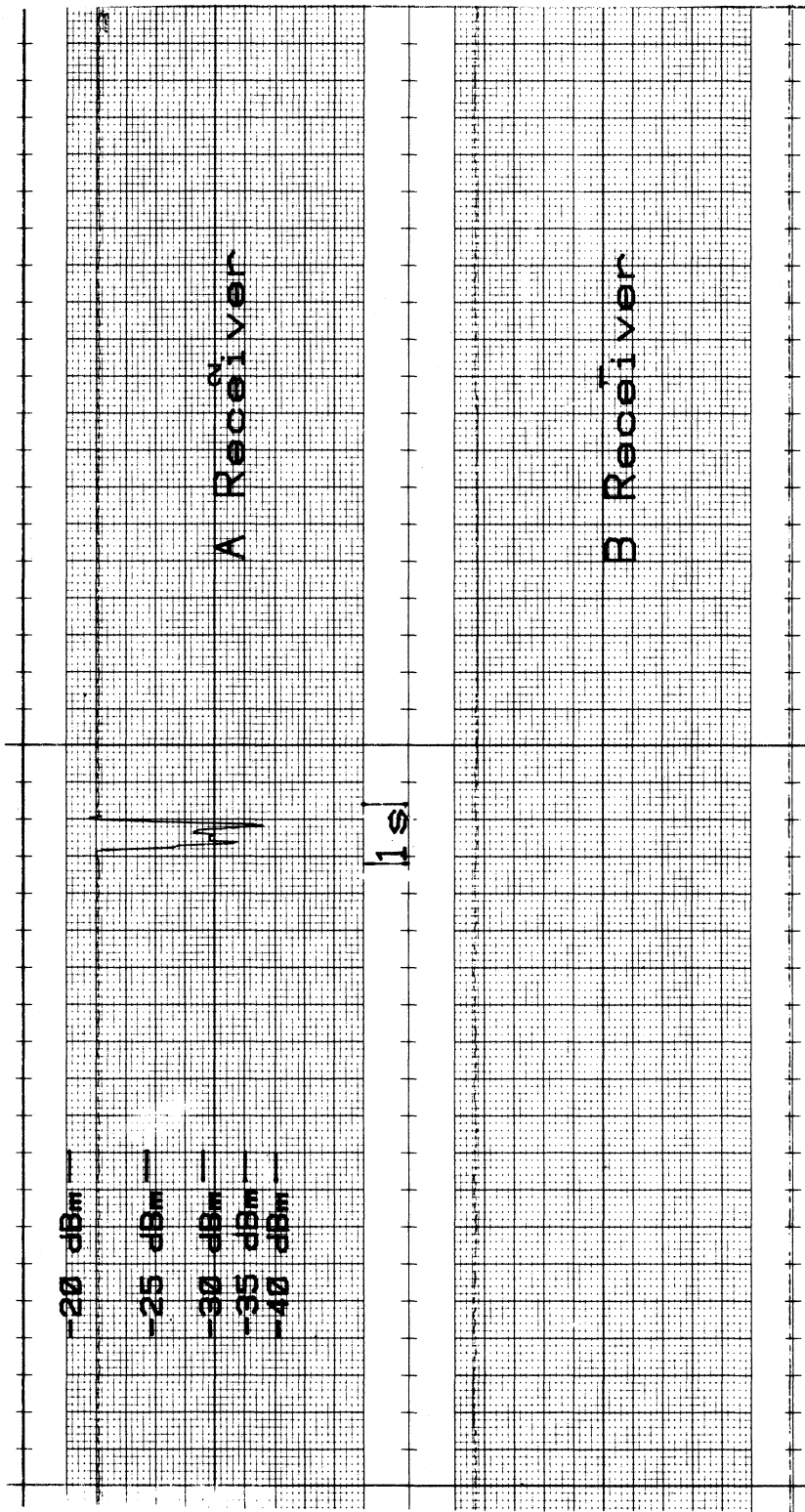


Figure 4.2. Aircraft fade (Atlanta).



Figure 4.3. Aircraft position in microwave path.



Figure 4.4. Aircraft position above microwave path.

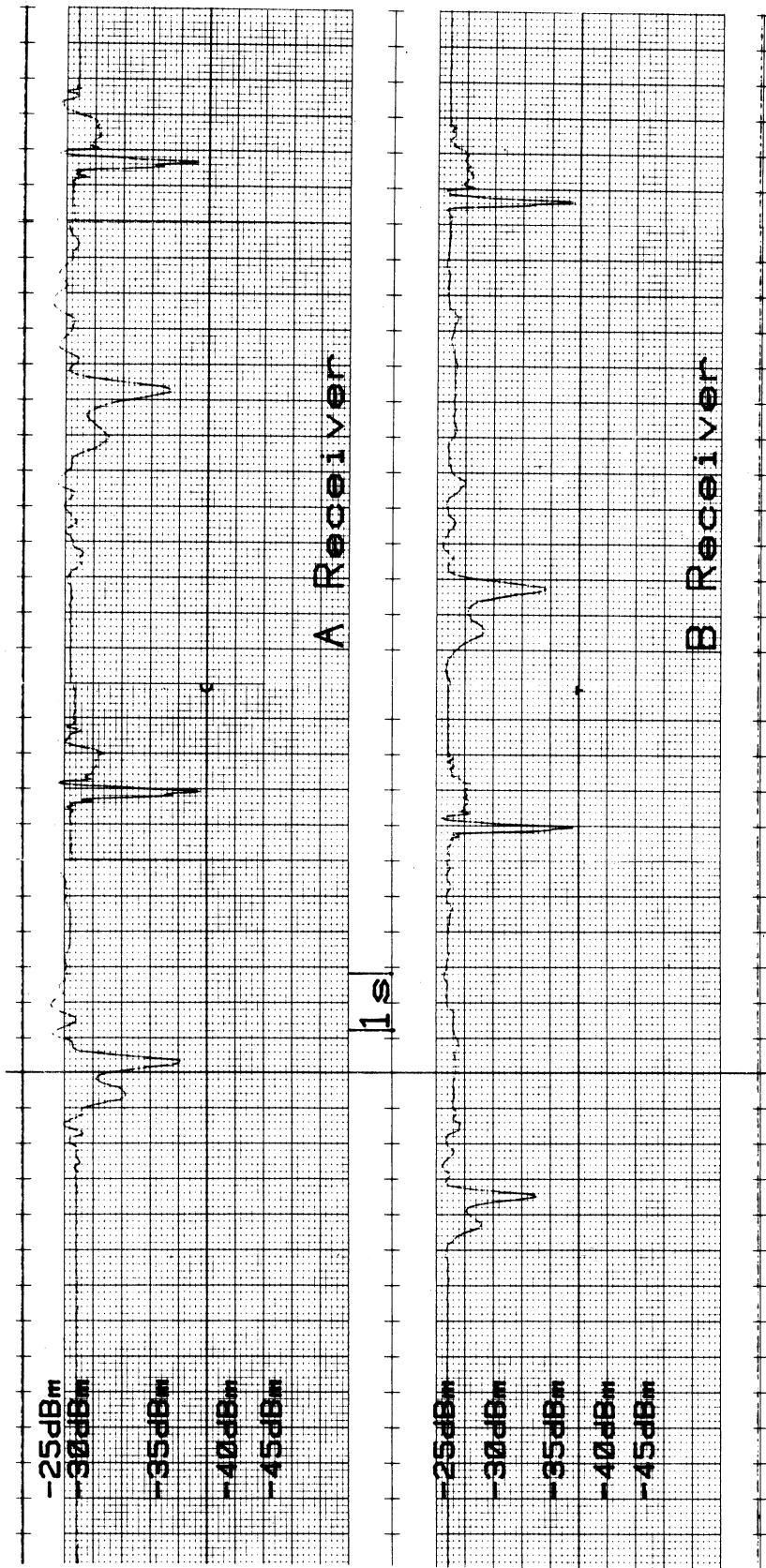


Figure 4.9. Multiple mixed fades at Chicago.

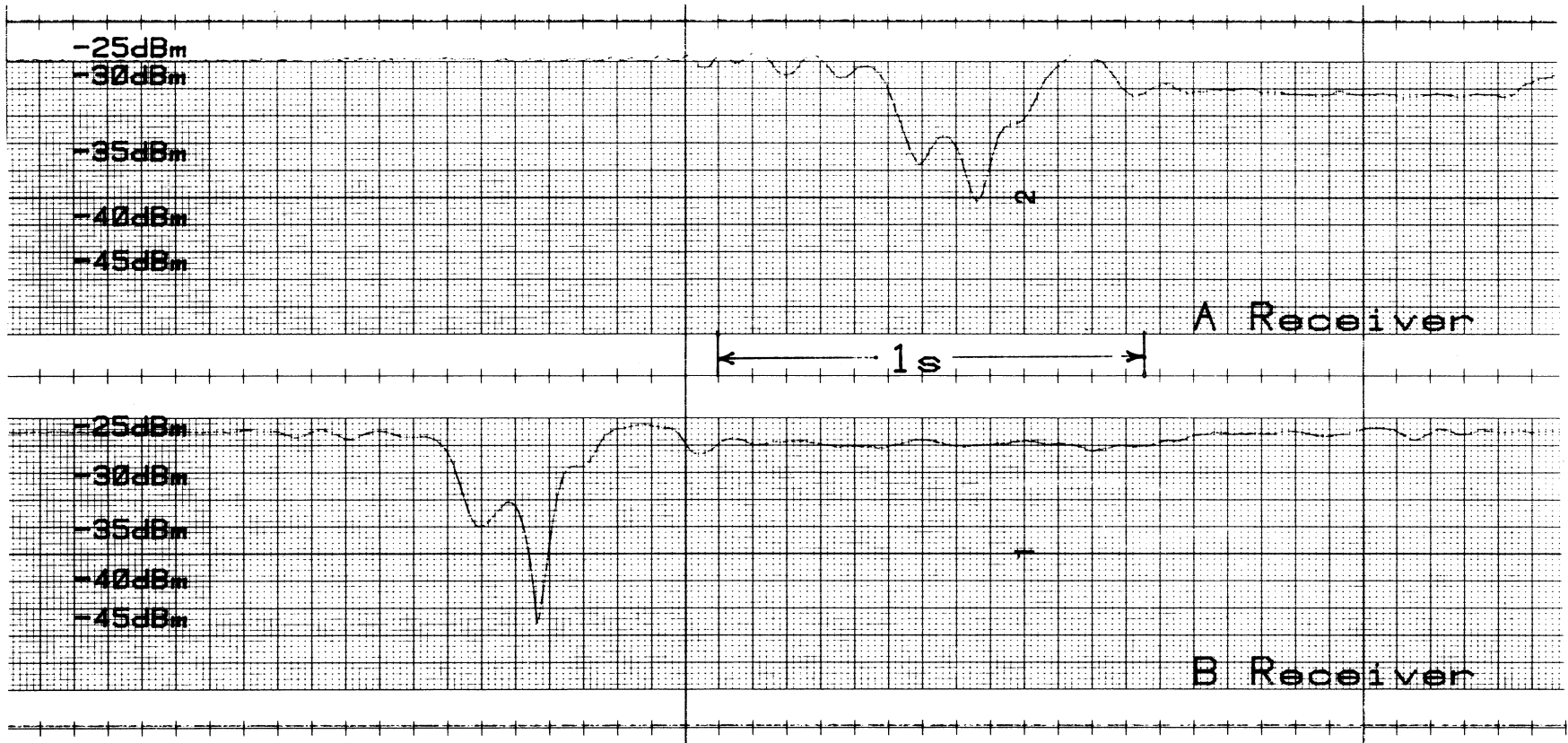


Figure 4.10. Time expanded fade at Chicago.

5.1. Hartsfield - Atlanta International Airport

The Atlanta airport has two microwave RML links as illustrated in Figure 2.1. The direct path crosses both runways on the south side between the radar site and the control tower. Due to a potential interference between the FAA operating frequency and the 8.6 GHz test frequency of the probe, it was not possible to instrument this link. Very little data could be obtained from this configuration in any event, since the arriving and departing aircraft were rarely in the microwave beam. They either passed under the beam on landing, or passed above the beam on takeoff.

The probe was installed on the reflected (Channel B) path, and the obstruction measurements were obtained from aircraft intercepting the reflected path between the water tower reflector and the control tower (see Fig. 2.1). This path proved to be almost ideal for the experiment, as landing aircraft approaching Runway 27R intersected the beam approximately 0.5 miles from the end of the runway. Occasionally, an aircraft approaching Runway 27L could also be observed, but these events were rare. Estimates of aircraft position, elevation, and speed on approach to Runway 27R would place them directly in the microwave path. This was also observed visually for most of the data obtained.

The traffic pattern on 14 July 1978 was such that most of the measured responses could be directly identified as to the type of aircraft.

All of the data for 14 July 1978 were played back from the magnetic tape recordings and scanned in the laboratory. No multipath was ever observed in the impulse responses from this configuration. Each aircraft caused only a power-fade response, with depths as reported in Section 4. The link itself displayed some slight ground reflections which are shown in Figure 5.1. The first surface reflection is seen as a distortion in the trailing edge of the response in this figure, and a smaller reflection is seen beyond the main response. The delay times are on the order of 3 ns and 7 ns respectively, as the base

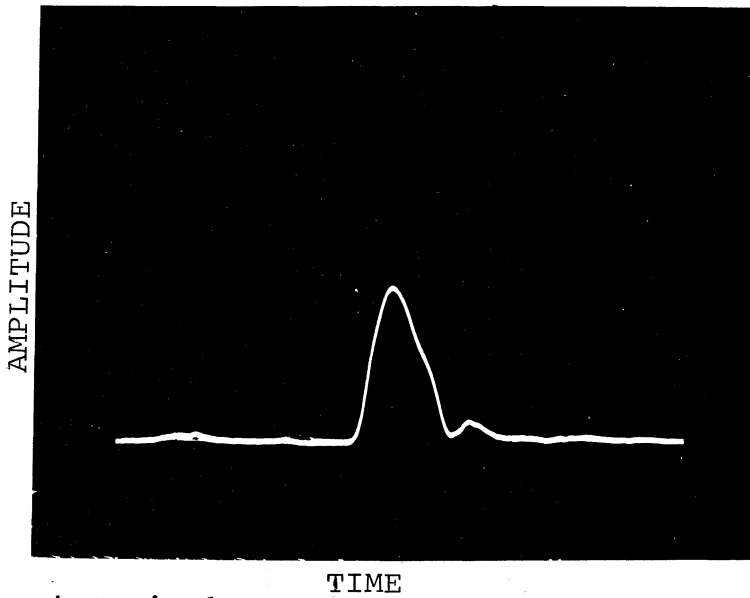
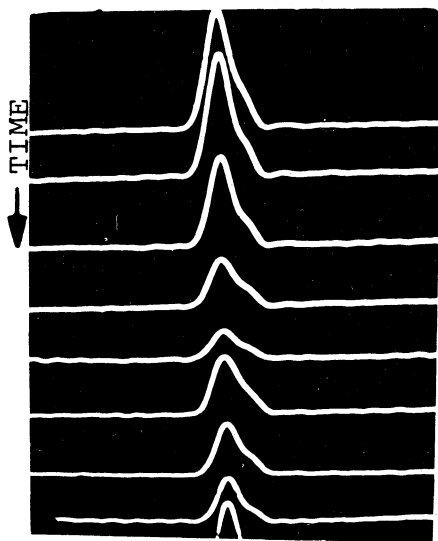
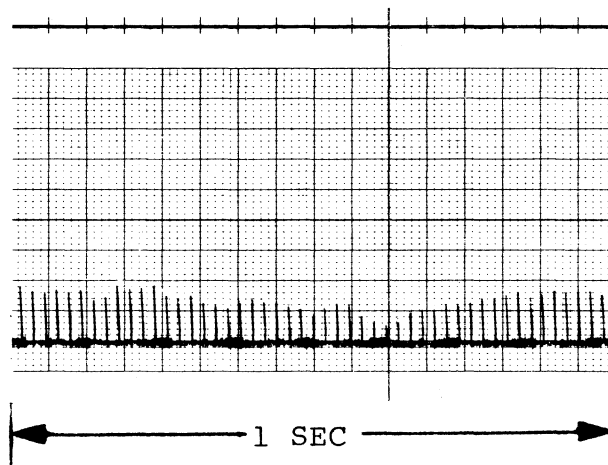


Figure 5.1. A typical response measured over the reflected (Channel B) link at the Atlanta airport without aircraft interference.



(a)



(b)

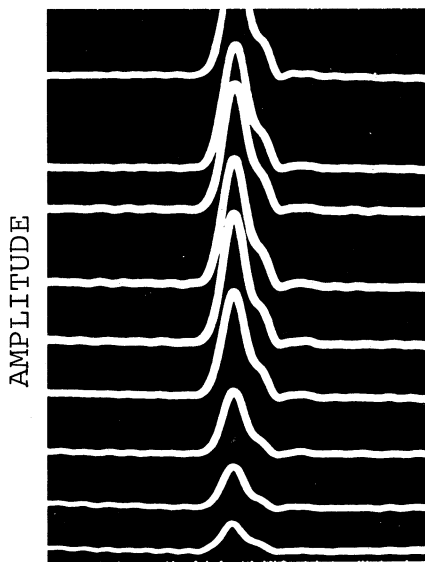
Figure 5.2. The impulse response measured at the Atlanta airport with a DC9 aircraft in the microwave beam. The time separation in (a) is 100 ms. The data rate in (b) 50 impulses per second.

width of a clear channel response would be 13.6 ns (1 cm in the figure). The response is linear in magnitude, so that the two reflected components are approximately -6 dB and -20 dB with respect to the direct response. These reflections are seen to be very stable in all of the following figures for the aircraft obstruction measurements.

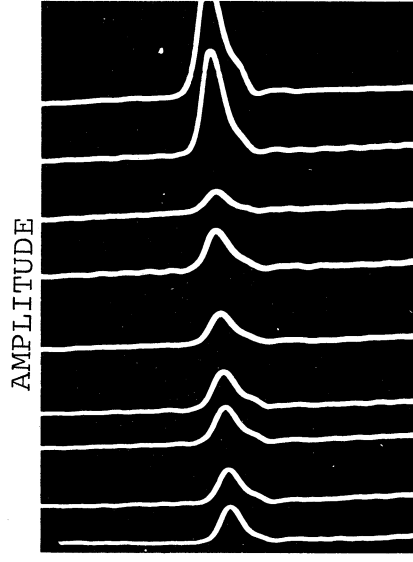
A typical response with an aircraft intersecting the reflected path (Channel B) beam is shown in Figure 5.2. Part (a) of this figure shows a time sequence of the impulse response observed when a DC9 aircraft was approaching 27R for a landing. The data rate was 10 impulses/s, so that the time between each response of this figure is 100 ms. A flat fade in the response is seen, which is on the order of 15 dB between the top trace and the fifth trace down. Note that the typical double null discussed in Section 4 is also visible in this response sequence. Part (b) of Figure 5.2 is a slow playback on a strip chart recorder of another measurement made later the same afternoon. The aircraft was again a DC9, and the envelope of the impulse response is seen to display the double null characteristic. The fade depth is less in this example than that in Part (a), and the data rate for this measurement was 50 impulses/s.

Figure 5.3 presents two more examples of the impulse response with obstructing aircraft in the beam. Part (a) is an example of the response where a 727 aircraft was on a landing approach to Runway 27R. Part (b) is an example of the response for a 727 aircraft that was on a landing approach to Runway 27L. In each case, we note the absence of any multipath with the exception of the surface reflected components noted for Figure 5.1. The sequence is not long enough in these photographs to illustrate the extent of the power fade in time. However, the duration of the fades were noted and discussed in Section 4. Note in example (a) however, that the double null is again evident from the sequence.

In all of the responses seen in Figures 5.2 and 5.3 that the magnitude relationship between the direct and surface



(a)



(b)

Figure 5.3. Examples of the impulse response measured at the Atlanta airport with 727 aircraft intercepting the microwave beam. In (a) the aircraft was approaching Runway 27R, and in (b) it was approaching Runway 27L. The time between responses is 100 ms in each case.

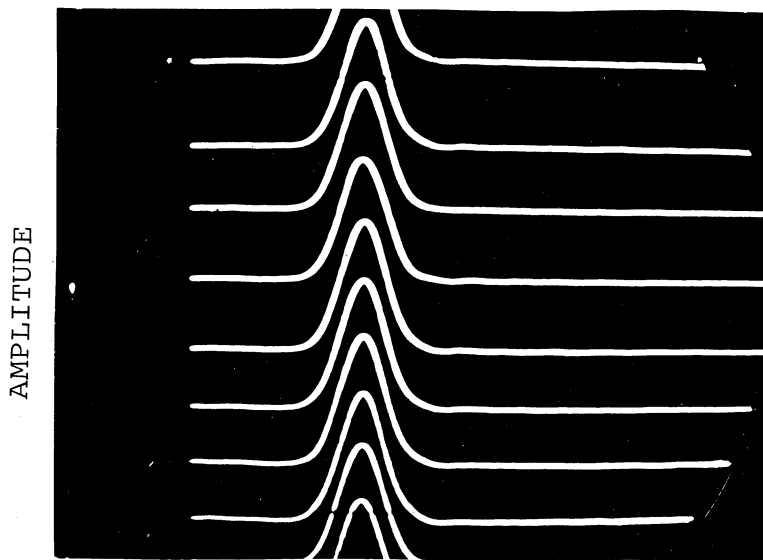


Figure 5.4. A sequence of impulse responses measured over the Chicago-O'Hare RML link with no aircraft interference.

reflection remains relatively fixed. This fact indicates that the surface reflection must lie between the radar site and the passive reflector since the aircraft would not normally disturb the reflection if it were on the reflected leg of the path.

From these measurements, we conclude that the obstruction of aircraft within the geometry for the Atlanta RML causes only a power fade to the microwave system. The absence of any multipath from the aircraft indicates that no frequency selective fading will result, and the performance of any digital system could be predicted on the basis of flat fading over the duration of the obstruction.

5.2. O'Hare - Chicago International Airport

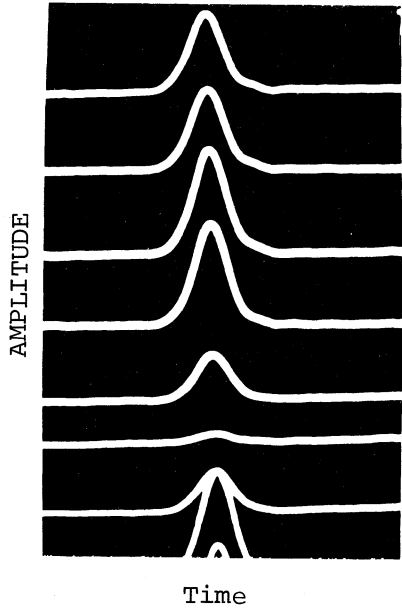
The two microwave links at Chicago O'Hare airport are side-by-side, providing a space diversity path as discussed in Section 2. The PN probe was installed on the northern-most link (Channel A) to minimize the potential interference to the FAA operating frequency. The most significant impulse response data were recorded on 19 July 1978, when the air traffic was operating on Runway 14R toward the southeast. The likelihood of obstruction by the entire aircraft on these links is much lower than that for the Atlanta airport, as noted in Section 2. Many more smaller disturbances were observed, probably due to the tail structures of aircraft penetrating the microwave beams when taxiing on the surface or when rolling on Runway 14R. However, a deep fade in the signal was observed occasionally. These deep fades have been interpreted as cases where the full aircraft has intersected the beam. Direct observation of the activity on the runway and taxiways was not possible due to the link configuration. This area was blocked from view at the receiver site (see Fig. 2.5).

The microwave path was essentially clear of any surface reflections, as shown in the sequence of responses in Figure 5.4. These responses are typical of a clear channel response, again with a base width of 13.6 ns and a time separation of 100 ms.

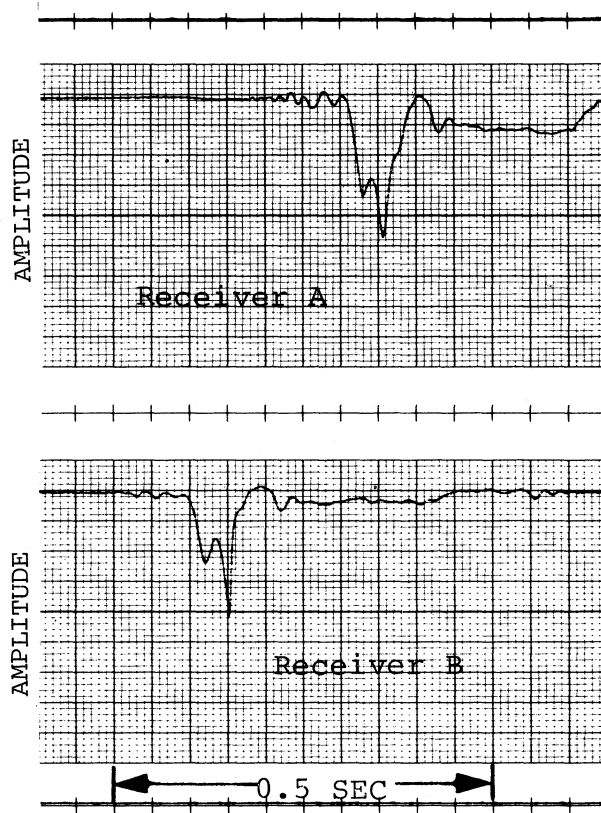
A complete scan of the impulse data recorded on 19 July 1978 was made in the laboratory. The deep-fade obstructions were found to display results quite similar to those observed in Atlanta. In general, the impulse response did not show any multipath when the aircraft was in the beam. A power fade with depths of the same order of magnitude as observed in the Atlanta data was the significant feature. However, occasionally a response was observed that contained a strong multipath component during an obstruction fade. This observation is discussed in more detail below, and a conclusion is given based on other observations from the data.

Figure 5.5 presents a typical response measured at Chicago-O'Hare. Part (a) presents a sequence of impulse responses recorded during the aircraft blockage shown in the accompanying record of the RML signal fade shown in Part (b). The impulse data correspond to the Channel A (upper) RML record. The fade is seen to extend over a period of approximately 100 ms, which is consistent with the impulse record where the separation between responses is 100 ms.

An example of a deep obstruction fade where multipath was observed is shown in Figure 5.6. The fourth response from the top of the photo displays a strong multipath component. The delay is between 3 and 4 ns, and the cusp in the response indicates that the component is near opposing phase with respect to the direct response. These features are discussed in greater detail in the appendix to this report. Similar cases were seen for a few other obstructions measured at O'Hare. To attribute the multipath to the aircraft causing the obstruction is contrary to all of the observations made at Atlanta, and to the majority of the obstructions measured at Chicago-O'Hare. In addition, the configuration for the Atlanta measurements would be more conducive to multipath from the obstructing aircraft since the flight path and the microwave path intersect at a more oblique angle. The possibility of a reflection from the vertical tail of the aircraft would be greater in the Atlanta



(a) Impulse response at 100 ms intervals.



(b) FAA/RML signal records.

Figure 5.5. A typical response measured over the Chicago-O'Hare link with an aircraft obstruction.

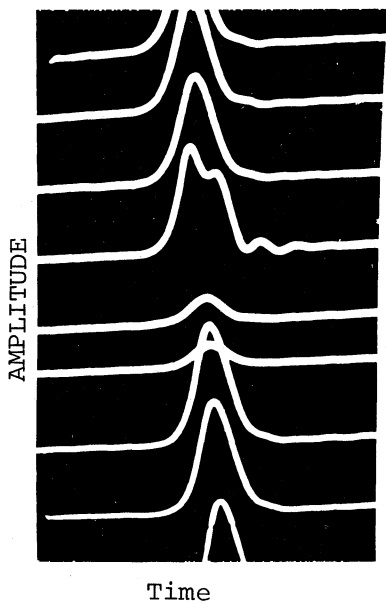
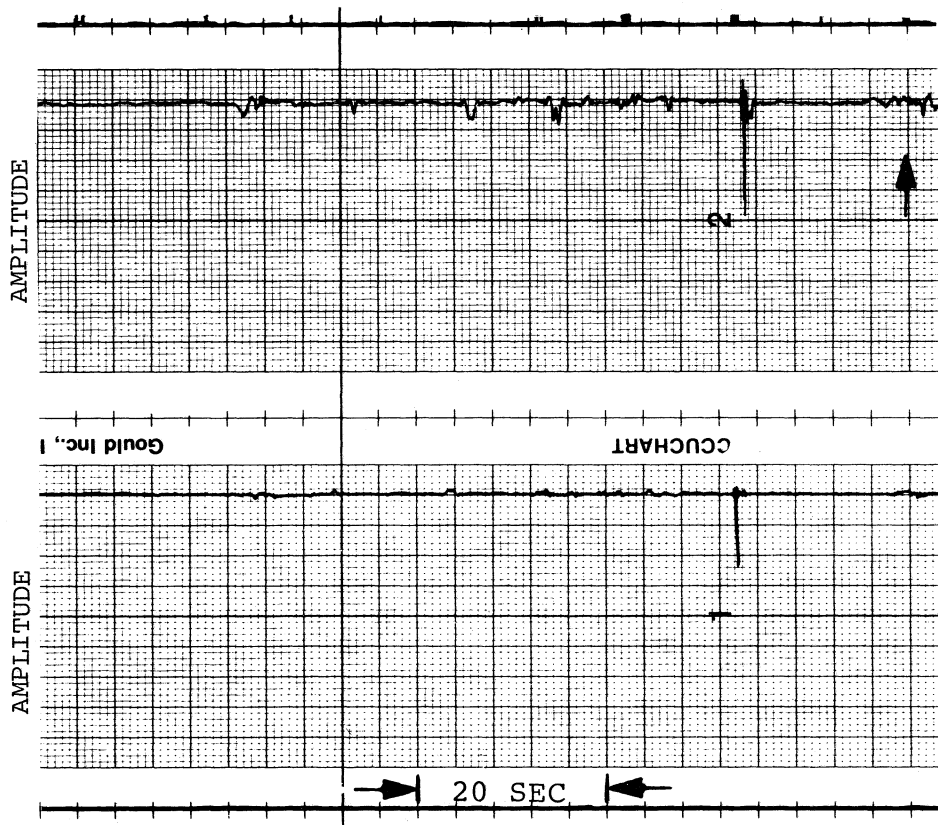


Figure 5.6. A sequence of impulse responses measured during an obstruction fade. Multipath is seen in the fourth trace from the top.

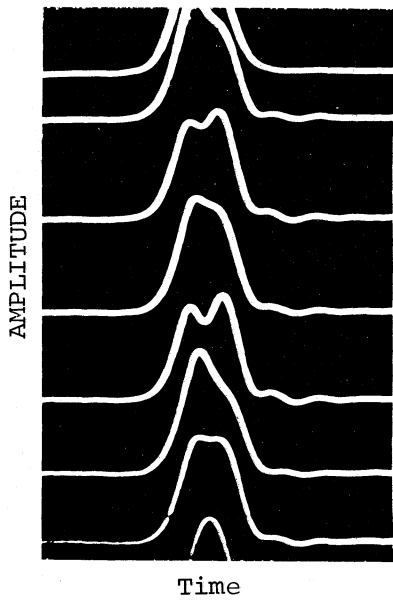
case than in the O'Hare configuration, where the intersect angle is nearly 45° . For these reasons, we do not believe this multipath was caused by the same aircraft that caused the deep-fade obstruction.

In order to determine the possible cause of the multipath, the data for the entire recording period at Chicago-O'Hare were played back from the magnetic tapes. The RML signals were transcribed on a strip-chart recorder, and the impulse response data were monitored on a storage oscilloscope. In this analysis, there were many cases of severe multipath observed in the impulse response at times when there were no (or only minor) disturbances seen in the RML records. Periods of observed multipath were flagged on the RML chart record using the event marker pen of the recorder. An example of this process is shown in Figure 5.7. Part (a) of this figure is a short section of the strip chart record showing periods of strong multipath that occurred both before and after a deep obstruction fade. Part (b) of the figure is a sequence of impulse responses measured approximately 15 s prior to the deep fade shown in (a). This sequence is typical of the multipath observed at other times, and the detail of the response is seen to be similar to that found in the one response shown in Figure 5.6. A close examination of the records for all of the O'Hare data indicates that any multipath seen during an obstruction fade was correlated with periods of multipath observed before and after the obstruction. For example, another event is illustrated in Figure 5.8. Note that very little multipath has been flagged on the RML record for this event, and the impulse response shown in (b) for the obstruction fade indicates no multipath.

As a result of the above analysis, we conclude that the multipath seen at O'Hare must be from aircraft moving on the surface of the airport, and not from the same aircraft that is directly intersecting the microwave beam. Using a mean delay of 4 ns for the primary multipath component, the ellipsoid for

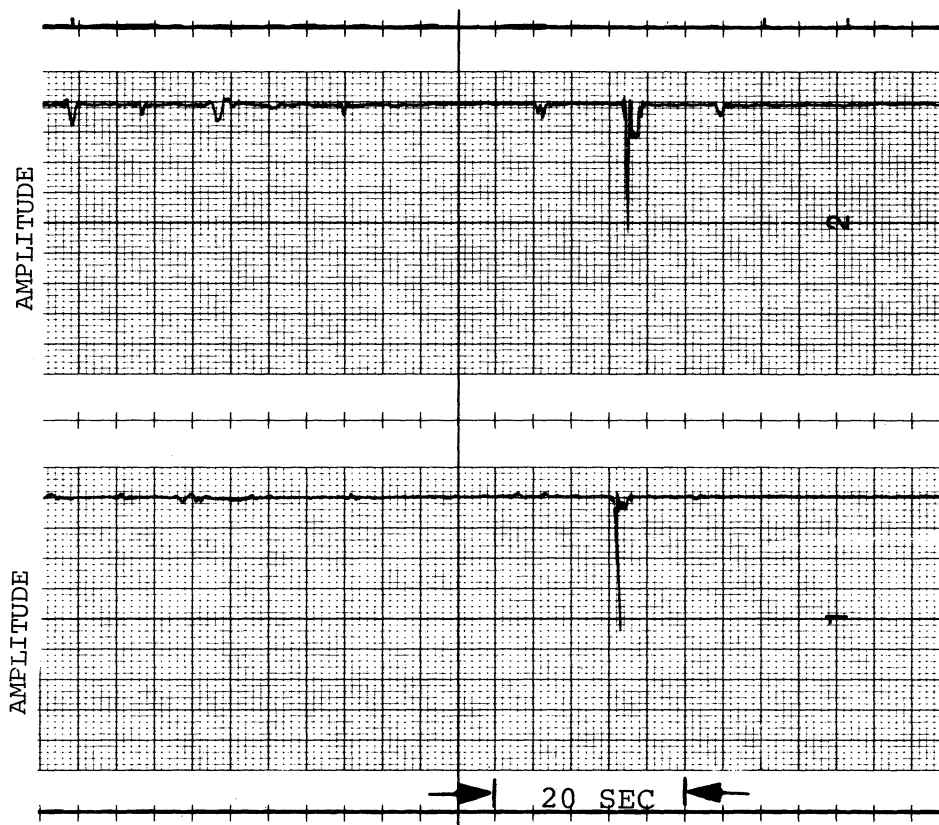


(a) Sample of the RML records where the times of observed multipath is indicated by the event marker (top trace).

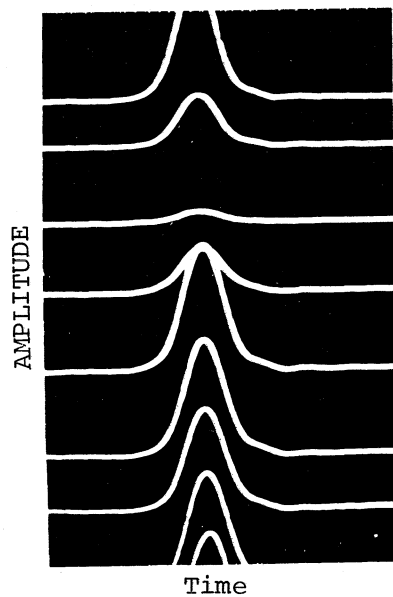


(b) An impulse response sequence measured at the time indicated by the arrow in (a).

Figure 5.7. Multipath observations over the Chicago-O'Hare link.



(a) A sample of the RML record where very little multipath was observed. Multipath was seen at times shown by the event marks in the top trace.



(b) The impulse response sequence measured during the deep obstruction fade in (a).

Figure 5.8. An obstruction fade without multipath.

the locus of the reflecting points can be drawn around the path shown in Figure 2.5. In the horizontal plane, the ellipsoid is on the order of 120 to 125 ft (36 to 38 m) on either side of the path at the location of the runway and two taxiways (see Fig. 2.9). It is noted that the tails of large jet aircraft are high enough to penetrate the microwave beam at any of these locations. The most likely origin of the multipath would be from aircraft on the inner taxiway and the terminal ramp area, as the orientation of the tail structure is more likely to be nearly parallel to the path. However, aircraft turning from the runway onto the two taxiways near the microwave beam could also produce the multipath. These conclusions are consistent with the data, but, of course, cannot be considered to be final or absolute.

The most important aspect of the multipath seen in the O'Hare measurements is its effect on digital transmission over a microwave circuit of this type. The multipath is severe enough to cause significant frequency-selective fading in the transmission channel of high data rate systems, with the associated degradation of the bit-error-rate (BER) performance.

These matters are discussed in more detail in the Appendix. The conclusion to be drawn is that extreme care must be taken in the design of such a microwave link. Even though approaching or departing aircraft on the runway appear to cause only a flat power fade when intersecting the beam, other aircraft on the surface of the airport could cause very significant problems to a digital transmission. The engineering for a link of this type must include adequate clearance for all surface aircraft and other structures.

6. CONCLUSIONS AND RECOMMENDATIONS

The primary objective of this program was to determine if aircraft obstruction of a microwave link was sufficient to cause a break in service to the subscriber. This program utilized two 8 GHz systems that were established by the FAA at

Atlanta and Chicago airports. The configuration examined was for aircraft in motion; i.e., take-off, taxi, or landing. The case of stationary aircraft was not addressed. The intent of the program was to determine if a problem may exist and to what degree rather than being a comprehensive, detailed measurement and analysis program in a controlled environment.

The results of this limited effort indicate that in a normal operational mode such as take-off, it is possible for aircraft to intersect a microwave beam and further to provide a degree of blocking sufficient to cause an observable signal fade. However, in the examination of nearly 200 cases, no fade was detected to exceed 20 dB and there was no indication of an enhancement of noise in the baseband to be of any concern. Systems designed with a 30 dB to 40 dB fade margin should more than tolerate the observed disturbances with no detectable degradation in customer service.

Having observed no pulse distortion at the Atlanta airport during the aircraft-caused fades indicates no frequency selective components within a 300 MHz bandwidth. This provides substantial support for the observed fades as being characterized as "flat" fades where the necessary band fades uniformly and equally. This fact minimizes any potential for baseband distortion or data stream disturbance.

There were also no observations at Atlanta of delayed pulses that would indicate discrete, strong multipath characteristics. This type of distortion could potentially cause second order effects on the data formats. Since there were none detected, confidence builds in stating that aircraft obstruction is not a significant problem. The test results indicate no significant first order effects that could cause baseband distortion. This does not preclude the existence of higher order, more subtle effects. This program did not address such problems nor did it eliminate the possibility of their existence.

On the other hand, some observations at the Chicago airport indicate a potential delayed component possibly caused by aircraft taxiing through a critical point on a system with low ground clearance. The detected delayed pulses were in the 3 to 5 ns range and relatively fixed. Two simple interpretations may be approached. As discussed in the appendix, the effect on a digital system operating with a 15 to 20 MHz bandwidth may be the distortion of the amplitude response to the degree of some asymmetry on the received spectrum. The effect of this asymmetry on digital system performance is not fully understood yet and requires additional experimental effort (discussed in more detail in the appendix.) A second simple view assumes that digital system intersymbol interference becomes excessive with delays greater than some fixed percentage of a bit interval (OT Tech. Memo 74-182, Farrow and Skerjanec, limited distribution). For the sake of this discussion consider a quarter of a bit interval to be the limit. With the 5 ns delay, the highest supportable data rate translates to 50 Mb/s. If the distortion criteria were one-half of a bit interval, the usable data rate becomes 100 Mb/s. This is to say that with the fixed delay detected at the Chicago airport and with the above assumptions, it may be possible to achieve a satisfactory system with data rates up to 50 Mb/s. These cases are for fixed phase differences and for a specific multiplex timing recovery system. These assumptions may be voided for variable phase cases and for other clock recovery and decision making technique.

From an engineering point of view certain criteria should be set in order to assure that the design choices are made to minimize the probability of intercepting an aircraft. Typically microwave links that traverse runways are short to the degree that variable atmospheric effects are negligible. The choice of terminal placement should be considered in light of minimizing the probability of intersection with aircraft movement. The terminal ends should not be closer than necessary to the nearest runway. The best choice would be across the middle of

a runway and avoiding paralleling of taxiways. Further, one should avoid crossing areas where aircraft stop while waiting for takeoff, gate access, etc. Finally, the terminal antennas should be sufficiently high to clear the tail section of the largest aircraft expected to operate at that airport. This is to exercise the available choices to assure the smallest probability of aircraft path and microwave path intersection.

System availability should not be affected by the shallow fades caused by aircraft. If the path is sufficiently short to not be affected by the atmospheric variability, diversity protection need not be considered for other than equipment availability.

7. ACKNOWLEDGMENTS

The authors wish to recognize the U.S. Army Communications-Electronics Engineering and Installation Agency for financial support for the program and in particular the personnel in the Electromagnetics Engineering Office at Ft. Huachuca, Arizona. We wish to thank the Federal Aviation Administration for granting access to and use of their communications systems. The cooperation and assistance were greatly appreciated from the Great Lakes Region and Mr. A. Qualiardi, O'Hare Radar/ARTS Section Chief and his personnel at Chicago and the Southern Region and Mr. J. Bryant, Manager, Airways Facilities Sector and his personnel at Atlanta.

8. REFERENCES

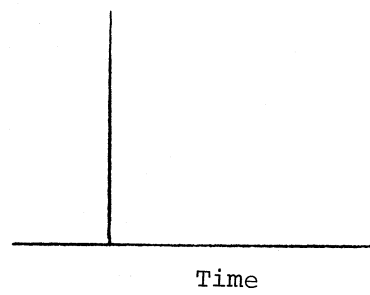
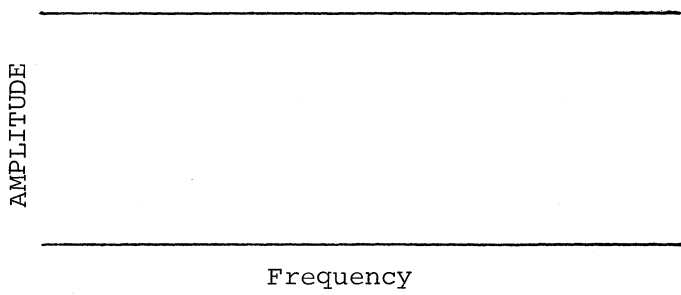
Linfield, R.F., R.W. Hubbard, and L.E. Pratt (1976), Transmission Channel Characterization by Impulse Response Measurements, OT Report 76-96, August.

APPENDIX - EXPLANATION OF IMPULSE TEST DATA

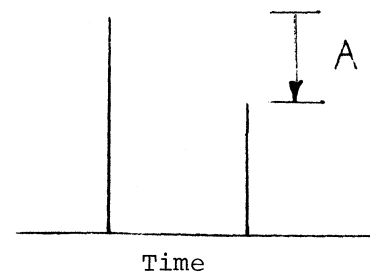
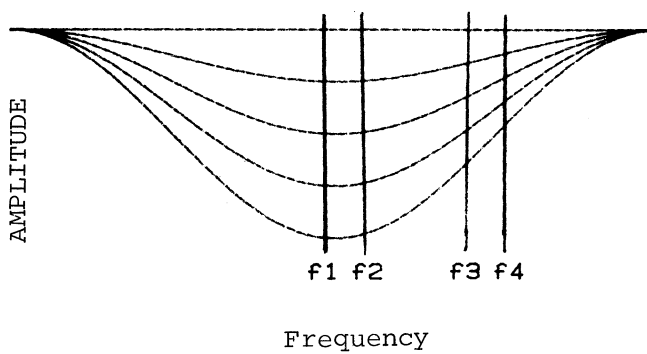
This section is provided to aid in the interpretation of the impulse test results and in the translation of these results to other systems. The primary objective of the ITS probe is to transmit a band of frequencies sufficiently wide to encompass a significant portion of a microwave band to allow detection of many of the shorter delays and distortions. The receiver portion of the system indirectly detects the amplitude response of the same frequency band.

In the ideal case, it would be desirable to transmit an infinitely short pulse such that its transform includes all frequencies as shown in Figure A-1(a). Figure A-1 contains in the right column a series of short pulses presented in the time domain. In the left column is the frequency spectrum corresponding to each pulse or pulse pair in the right column. The amplitude, frequency, and time scales are not shown since the figure is for illustrative purposes only. If the two pulses maintain a fixed delay but their amplitudes vary with respect to each other, the depth of the null or nulls in the spectrum will vary as displayed in Figure A-1(b). As the difference, A , increases, the spectral null becomes shallower. If, on the other hand, there are two pulses present separated by some time delay T , the spectrum will be sinusoidal in shape as shown in Figure A-1(c). If the relative amplitudes are fixed, but the time delay, T , allowed to change, the null positions change and become more dense as the time delay increases. This is illustrated in Figure A-1(c).

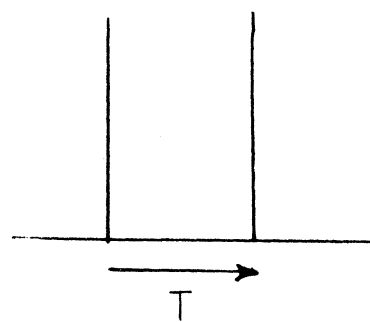
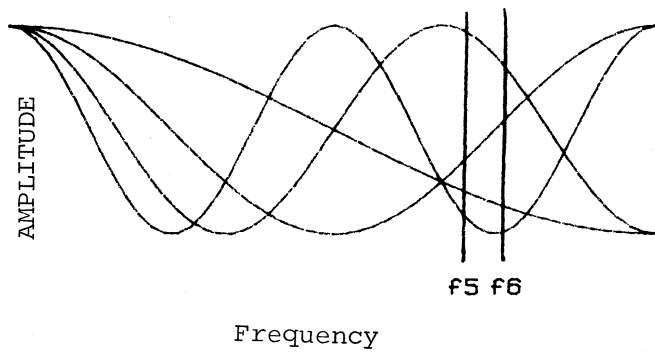
The discussion to this point has been for very wide bandwidths. Even for a pulse with a finite width such as that realized from the ITS probe, the bandwidth is approximately 300 MHz. The question at this point is what such a measurement would tell about a system operating with a bandwidth of 10% of this value or less. This may be illustrated by the frequency bands superimposed on the spectra in Figure A-1(b) and (c). If



(a)



(b)



(c)

Frequency Domain

Time Domain

Figure A-1. Time and frequency domain displays.

the operating digital system were constrained between f_1 and f_2 , the system would experience fading that would have the appearance of flat fading. The amplitude response in this case can be seen to be flat, or nearly so, and symmetrical. If the system limits were between f_3 and f_4 , the fading would not be as deep as the previous case but the pass band would contain a sloped response as a function of frequency and would be asymmetrical. Finally in the third case, Figure A-1(c), a system operating between f_5 and f_6 would experience sloped amplitude responses with changes in direction of the slope as well as change of direction within the band. In the latter two cases, the fading is frequency dependent in that all frequencies are not attenuated uniformly. Finally a fourth case can be imagined that consists of varying time delays and relative amplitudes so that one has a combination of those effects illustrated in Figure A-1(b) and (c). This in fact may be the case in most physical situations when multipath is a problem.

The effect of this frequency variable response within the passband of a receiver and detector is not fully understood yet. Experimental efforts are underway at Bell Labs and Collins Radio (Barnett, 1978; Rockwell International, 1978) to determine a quantitative measure in terms of bit error rate performance as a function of the slope of the frequency response. Considerable experimentation and analysis is still necessary to provide sufficient engineering guidelines to cope with such problems.

In order to provide some indication of the impact of the multipath observed at Chicago-O'Hare airport, we present the following brief analysis. In this development, we will refer to the generalization presented (where possible) with values from the measured data.

The mean value of the delay of the multipath component was measured to be 2 to 4 ns. Also the delayed signal was approximately of the same magnitude (and sometimes greater in magnitude) as the more direct signal. As an illustration, we choose

to model this transmission channel as a two-path channel with equal magnitudes for the two paths. Thus, the impulse response would be that illustrated in Figure A-1(b) where $A=0$ and the delay $T=2$ to 4 ns. The Fourier transform of the impulse response yields the frequency transfer function $H(f)$ of the channel. The transform in this case is a sinusoid as illustrated in Figure A-1 with a frequency period of 500 MHz for $T=2$ ns and 250 MHz for $T=4$ ns. On a logarithmic power scale, this transfer function is similar to a cycloid with deep nulls along the frequency axis as illustrated in Figure A-2. The location of the nulls is given by

$$f_n = n/T \tag{A-1}$$

where n is an integer (>0), and is odd for a reflection with phase reversal and even for a delayed component in-phase with the direct path. For the case considered here, where the reflection is assumed to be from the surface (or tail) of an aircraft on the airport ramp or taxiways, the reflection would have a phase reversal, and n would be an odd integer. The spacing between frequency nulls is given simply from

$$\Delta f_n = 1/T. \tag{A-2}$$

Let us assume an operating frequency for the microwave link to be 7.4 GHz. We first need to determine where the frequency nulls of $H(f)$ fall with respect to the operating frequency. Using (A-1) for a value of $f_n = 7.4$ GHz and; a delay of 2 ns, we find that n must have a value of 15. Thus, the nearest null to the operating frequency is found as

$$f_n = \frac{15}{2 \text{ ns}} = 7.5 \text{ GHz}, \tag{A-3}$$

and subsequent nulls will occur at 500 MHz intervals. The value of n corresponds to the Fresnel zones; in other words, the reflection at 7.5 GHz in the channel would be from the 15th Fresnel zone ellipsoid.

In a similar manner, we find that for a delay $T=4$ ns, the transfer function $H(f)$ has a null at $f_n = 7.25$ GHz ($n=29$).

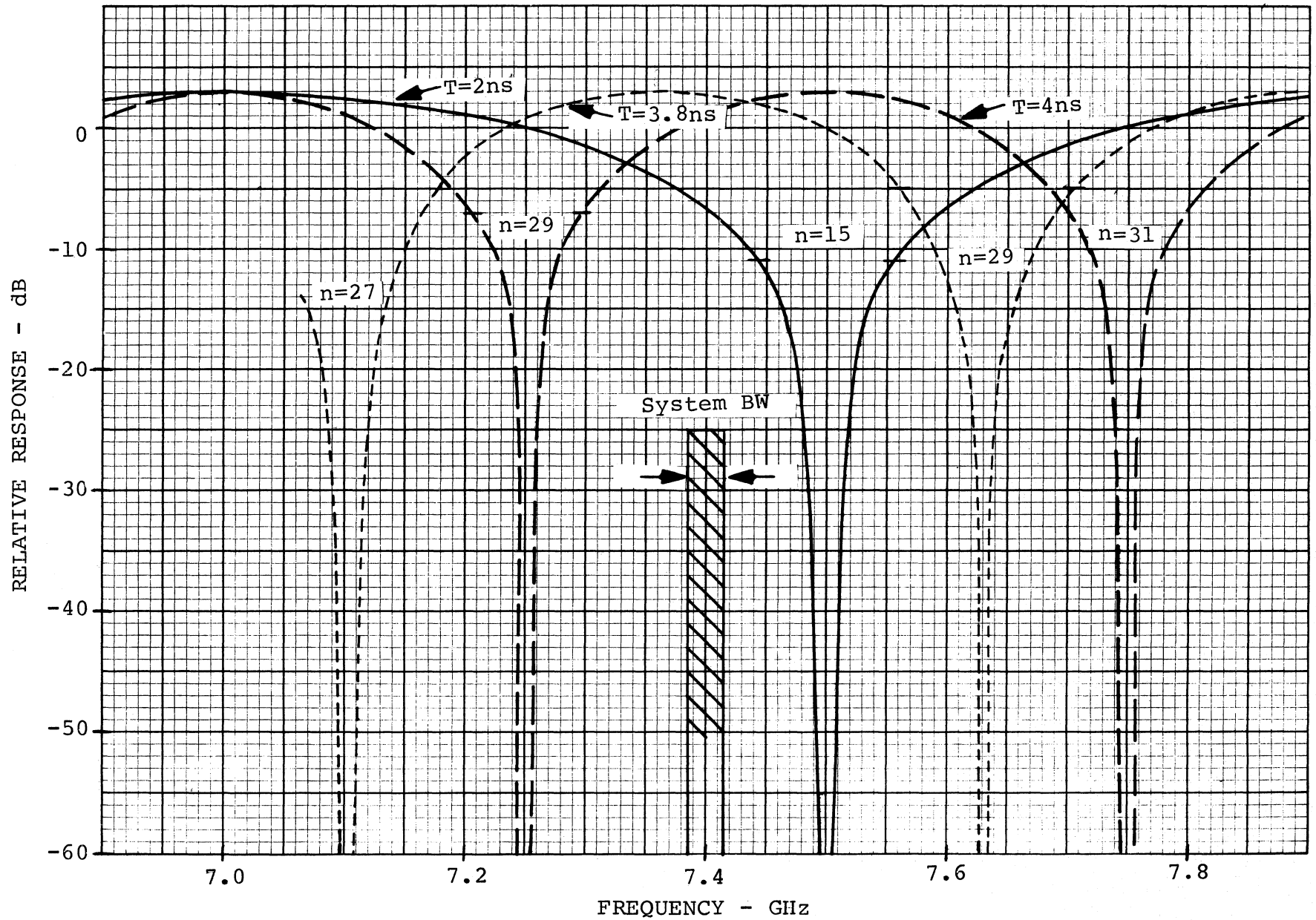


Figure A-2. The theoretical transfer function of a multipath channel.

This transfer function has a null-spacing of 250 MHz. Both of these channel functions are plotted in Figure A-2, identified by the value of the integer n and delay time T . Also drafted on this figure for illustration is the signal spectrum of the microwave system at the 7.4 GHz operating frequency. We have assumed a spectral bandwidth (BW) of 30 MHz, typical of a digital transmission system operating in this frequency band.

At first glance, one might conclude that the multipath structure considered here, which results in the frequency transfer functions of Figure A-2, would have little or no effect on the operating system. In a static situation, this conclusion would be correct. The transmission channel in both cases would cause only minor distortions across the signal spectrum. The operating system is well removed in frequency from the deep nulls in the transfer functions, and the frequency selective fading within the signal BW is at most 2 dB across the BW. This aspect of performance degradation in a digital system does not become critical until the spectral slope distortion becomes considerably greater. This matter is discussed in more detail below.

The most critical consideration in the multipath structure which we have depicted is a result of the dynamics of the channel. For example, the physical situation we are modeling here involves reflections from moving aircraft. Thus, the channel transfer function is not static, but becomes a time-variant or dynamic function; a time-variant filter in our communication system. For the conditions shown in Figure A-2, let us assume that the reflection point (on a moving aircraft) has changed positions over a short time span such that the original delayed component shifts from a delay of 4 ns to 2 ns. The frequency transfer function in the dynamic view becomes very difficult to depict; however, it can be visualized as "elastic". For example, consider the functions in Figure A-2 as stretching or relaxing in an elastic fashion. The nulls of the function thus change position along the frequency axis, and the shape of the function changes. As can be seen in Figure A-2, the slope of

the function as it approaches the cusp of a null will also change. In addition to this dynamic change, we must keep in mind that the value of the integer n is also changing as the time delay changes. The dynamics of this change can be visualized by considering the entire $H(f)$ function shifting along the frequency axis either to the right or left. This change is most critical in considering the dynamic effects on system performance. For example, if we assume a slight change in delay-time from 4 to 3.8 ns, the frequency transfer function of the channel shifts between the two dashed-line functions in Figure A-2. Note that the null corresponding to $n=29$ in these two functions has moved from 7.25 GHz to 7.63 GHz. Thus, this null has passed through our system pass-band as the time delay changed. In the case we are modeling here, we note that the latter change will cause a frequency null to pass through the operating system BW a total of 8 times as the delay changes from 4 to 2 ns. This will obviously cause severe frequency selective fading within the signal bandwidth, as well as power fading across the complete BW during times when the null or cusp of the filter characteristic passes our operating frequency. The rate at which the distortions impact on the signal BW is a direct function of the rate at which the time-delay between the signal components changes. However, it is also important to observe that even if the time-delay change is linear with time, the rate of change in the frequency transfer function is non-linear. For example, if the time delay is changing from 2 ns to 4 ns (increasing) the initial nulls that pass the operating frequency will do so at a higher rate per unit time than the later ones.

The actual impact on (degradation of) a microwave digital transmission system, caused by the multipath structure considered above, is very difficult to assess analytically. To begin with, the resulting bit error rate (BER) will depend somewhat on the type of system used and on the actual digital transmission rate. A simplified view of the transmission rate

dependence can be gleaned by considering a 5 MHz signal BW in Figure A-2 in comparison with the 30 MHz shown. It is obvious that the frequency selective distortions would be less severe in a 5 MHz BW, and the frequency nulls would cause fading across the signal BW that more nearly resemble power or attenuation fading. Most digital systems will perform differently under these two classifications of signal distortions. The most straightforward techniques that can be used to evaluate system performance under varying channel conditions, and different system characteristics and parameters, would be through laboratory simulation processes. Without benefit of such studies, or actual digital system tests in the multipath channel, it is almost impossible to predict the performance under the dynamic conditions measured or postulated for the microwave link at Chicago-O'Hare airport. However, the multipath observed over this link occurred a significant amount of time, and the impact on a digital transmission link can be gleaned from the discussion given below.

Based on the measurements made and presented in this report, the most important recommendation that can be made is that the proposed microwave links be engineered and tested so that they exclude any possibility of multipath interference on the airport surface. Measurement results from the Atlanta airport indicate that multipath is not a problem with aircraft in the microwave beam; at least within the geometries of the two test configurations. Thus, the important criteria is to avoid the surface type multipath observed at Chicago-O'Hare.

There have been some recent efforts to determine the degradation caused by frequency selective fading to a digital system. Even though these measurements are made only in a static or semi-static sense, they are significant enough to report here. With respect to actual over-the-air performance tests, Barnett (1978) has reported results that convey the importance of frequency selective fading, or what Barnett terms the in-band linear amplitude dispersion. In his measurements,

Barnett used a number of narrow-band (slot) filters within the signal BW of a 78 Mb/s, 8 PSK system, operating at 6 GHz. Observing the power in the two filters at the extremities of the pass-band provides a rough measure of the amplitude dispersion caused by the characteristic of the frequency transfer function of the channel. He reported that a slope on the order of 0.2 dB/MHz across the BW of his system was sufficient to cause the BER performance to degrade to 10^{-3} , or below this threshold value. An in-band slope of this value (or greater) would occur for the cases shown in Figure A-2 below the levels marked with the short cross-lines. Thus, for example, if the transmission of interest were operating at 7.45 GHz in a static channel that has either of the response characteristics shown in Figure A-2, the performance would be degraded to the order reported by Barnett. It thus becomes clear that the performance in a dynamic channel can only be treated on a statistical basis. The measurements performed in the current project at Atlanta and O'Hare airports do not form a statistical sample that is sufficient to predict long range performance. The fact that a dynamic multipath structure was observed is, however, sufficient to raise a genuine concern, and to serve as a cautionary example in the design of future digital systems in an airport environment.

It should be pointed out here that the synopsis given in this Appendix applies only to a single non-diversity link, and one which uses no other adaptive process. It has been shown (Anderson, et al., 1978; Rockwell International, private communication, 1978) that both space diversity and some form of adaptive equalization in the microwave receiver can significantly improve the system performance in multipath environments. However, detailed studies need to be made under controlled dynamic conditions (preferably simulated) to document the potential improvements that have been observed under quasi-static conditions.

A step beyond understanding the foregoing effects is the need to know the frequency of occurrence, the duration of such

occurrences, and its total impact on system availability. The effects discussed above are not continuous occurrences but rather appear somewhat infrequently and are of short duration. In short, there is a time factor that weighs heavily in the determination of system impact.

REFERENCES

- Anderson, C.W., S. Barber, and R. Patel (1978), The effect of selective fading on digital radio, International Communications Conference, Toronto, Ontario, Canada, June.
- Barnett, W.I. (1978), Measured performance of a high capacity 6 GHz digital radio system, International Communications Conference, Toronto, Ontario, Canada, June.



BIBLIOGRAPHIC DATA SHEET

		1. PUBLICATION OR REPORT NO. NTIA Report 79-14	2. Gov't Accession No.	3. Recipient's Accession No.
4. TITLE AND SUBTITLE Aircraft Obstruction of Microwave Links			5. Publication Date January 1979	
			6. Performing Organization Code	
7. AUTHOR(S) R.E. Skerjanec and R.W. Hubbard			9. Project/Task/Work Unit No. 9103533 9103534	
8. PERFORMING ORGANIZATION NAME AND ADDRESS National Telecommunications and Information Administration, Institute for Telecommunication Sciences, Boulder, Colorado 80303			10. Contract/Grant No.	
11. Sponsoring Organization Name and Address USACC/CEEIA Fort Huachuca, AZ			12. Type of Report and Period Covered NTIA Report	
			13. Final	
14. SUPPLEMENTARY NOTES				
15. ABSTRACT (A 200-word or less factual summary of most significant information. If document includes a significant bibliography or literature survey, mention it here.) Conversion to digital transmission has renewed the concerns about what effects aircraft obstruction of microwave links have on user quality. This is of particular concern where it is necessary to install a telecommunication system that crosses runways and taxiways where the frequency of obstruction may be great. A limited measurement program at 8 GHz at Atland Chicago Airports was undertaken to determine if a condition existed that could cause exces error rates on digital systems. Measurements were made of the received signal level together witthe impulse response of the transmission medium. (Continued)				
16. Key Words (Alphabetical order, separated by semicolons) Microwave propagation; impulse response; digital transmission; aircraft obstruction				
17. AVAILABILITY STATEMENT <input checked="" type="checkbox"/> UNLIMITED. <input type="checkbox"/> FOR OFFICIAL DISTRIBUTION.		18. Security Class (This report) Unclassified		20. Number of pages 68
		19. Security Class (This page) Unclassified		21. Price:

15. ABSTRACT (Continued)

Measurement results indicate that during takeoff and landing, aircraft can cause signal level fades to 20 dB. Modern system margin is usually sufficient to cope with such fades.

The impulse response measurements at Atlanta did not reveal any delayed or distorted pulses that would indicate excessive multipath and frequency selective fading. However, slight distortion from taxiing aircraft at Chicago was observed. The implication of this detected distortion is reflected in the potential of a distorted asymmetrical frequency response within the 15 - 20 MHz passband of a microwave digital receiver.